

Acetate-Enriched Substrates for Enhanced Methane Production in Anaerobic Systems

Quirin Königbaur

Degree project/Independent project • 30 credits Swedish University of Agricultural Sciences, SLU Department of Molecular Sciences Environmental science Molecular Sciences, 2025:28 Uppsala, 2025

Acetate-Enriched Substrates for Enhanced Methane Production in Anaerobic Systems

Quirin Königbaur

Supervisor:	Jonas Ohlsson, Swedish University of Agricultural Science, Department of Molecular Sciences			
Co supervisor:	Alexander Bauer, University of Natural Resources and Life Sciences, Institute of Agricultural Engineering			
Examiner:	Anna Schnurer, Swedish University of Agricultural Science, Depart-			
	ment of Molecular Sciences			
Credits:	30 credits			
Level:	A2E			
Course title:	Master thesis in Environmental science			
Course code:	EX0897			
Programme/education: EnvEuro				
Course coordinating dept:	Department of Molecular Sciences			
Place of publication: Uppsala				
Year of publication: 2025				
Title of series:	Molecular Sciences			
Part number:	2025:28			
Keywords:	Biogas, Acetate, TBR, CSTR, Hydrogen, VFA, Anaerobic			
- y	Digestion, PtG			

Abstract

A transition in the current energy system is needed for multiple reasons. For example, fossil fuels are depleting and have a major impact on the climate. A shortage of renewable energies, under and over production at peak times are examples of the challenges the industry/research are facing today. Current research shows that Hydrogen can be a component to renewable energy integration, and thus a positive component in the energy transition towards a sustainable and stable power supply. However, producing hydrogen requires large amounts of electric energy, but can't be easily stored.

To facilitate transportation and storage, hydrogen can be converted into organic acids. Primarily acetic acid with a process that incorporates carbon dioxide and hydrogen in a trickle-bed reactor. It is known that acetic acid plays a key role in biogas plants, where it contributes to methane generation. This thesis explores the conversion of hydrogen into organic acids under different environmental conditions to identify the factors that achieve the highest production rates. The resulting liquid product is then tested as a substrate in a biogas reactor, and its impact on gas production is compared with that of two reference reactors.

Through the analytical methods used in this research—including measurements of volatile fatty acids, gas composition, gas flow, temperature, and pH—it was shown that, at its peak, the trickle-bed reactor achieved an acetic acid concentration of 12.4 g/L with a maximum production rate of 3.83 g/L per day. The process performed better at higher pH values around 9 compared to lower pH values around 6. Using this acetate substrate, methane gas production in the biogas reactor was 36% higher than in the reference system over one retention time. The results show that higher pH levels in the trickle-bed reactor improve the conversion of hydrogen to acetic acid and increase methane production, supporting its use in microbial Power-to-Gas solutions and as renewable energy storage.

Keywords: Biogas ,Acetate ,TBR ,CSTR ,Hydrogen ,VFA ,Anaerobic digestion, PtG

Popular science summary

Climate change, fossil fuel shortages, and recent global conflicts have shown how urgently our energy system needs to change. Renewable energy is part of the solution, but it doesn't always produce power when we need it. At times, there's too much electricity — especially from wind and solar — that ends up going unused.

This research looks at how that extra energy can be put to better use. One promising idea is to use surplus electricity to produce hydrogen, a clean energy carrier. But hydrogen is tricky — it's expensive to produce, hard to store, and not easy to transport.

To solve this, the thesis tested a way to convert hydrogen into acetic acid, a liquid that's easier to handle. The process combines CO₂ and hydrogen in a trickle-bed reactor, a system where gas flows through a bed of liquid-coated material. Acetic acid is more than just a storage option — it's also valuable for biogas plants, where it helps boost methane production.

The study explored how different environmental conditions — especially pH — affect how efficiently hydrogen turns into acetic acid. It found that the reactor worked best at a pH of around 9, reaching a maximum concentration of 12.4 grams per litre and a daily production rate of 6.36 grams per litre.

To test their use for biogas plants, the acetic acid was added to a working biogas reactor. With that the methane gas production increased by 36% compared to the two reference reactors. The quality of the gas was also improved.

Acknowledgement

I would like to begin by expressing my sincere thanks to everyone at the Department of Molecular Sciences, Swedish University of Agricultural Sciences, for creating a supportive and inspiring research environment throughout my thesis work.

I am especially grateful to my supervisor, Jonas Ohlsson, for his invaluable support, guidance, and dedication during this project. His expertise and encouragement were instrumental to the successful completion of this work. My sincere thanks also go to Anna Schnürer, who supported as the examiner, for her insightful feedback and valuable input throughout the process. A special thanks to Simon Isaksson for the excellent collaboration in the laboratory — thank you for the great teamwork!

In addition, I would like to thank my family, friends, and fellow students for their mental and emotional support throughout this journey. A special thanks goes to Cato Debrabandere, Hamza Shaheen, and Emmanuella Kwakye for their encouragement and companionship.

This thesis would not have been possible without your collective support, knowledge, and shared enthusiasm for the subject.

Table of contents

Abst	tract	i
Popu	oular science summary	ii
Ackr	nowledgement	iii
List	of figures	v i
	of equations:	
	of tables	
	of appendixes	
	••	
Abbi	previations	
1.	Introduction	
1.1	Biogas and climate change	
1.2	Hydrogen	1
1.3	Anaerobic digestion	
1.4	Power to gas	4
1.5	Relationship between acetogens and methanogens	5
	1.5.1 Promoting acetate formation over methanogenesis	
1.6	Aim and Research Question	6
2.	Material and Methods	7
2.1	Design and Function of the TBR	9
2.2	CSTR Setup and Operation	11
2.3	Process Monitoring and Analysis	12
	2.3.1 Biogas 5000	12
	2.3.2 Gas chromatography	12
	2.3.3 FOS/TAC	13
	2.3.4 High-performance liquid chromatography	13
3.	Result	14
3.1	TBR	14
	3.1.1 Comparison between TBR1 and TBR2	14
	3.1.2 Comparison with literature	16
	3.1.3 Acid composition in TBR	18
	3.1.4 Process Disturbances and Contamination	20
	3.1.5 Gas Compositions	21
3.2	CSTR	22
	3.2.1 Calculation gas production	22
	3.2.2 Methane Production in CSTRs	24
	3.2.3 Volumetric methane production	25

4.	Discussion	27
4.1	Utilizing Acetate-Rich Substrates in CSTR	27
4.2	Performance Constraints and Enhancements in TBR	28
4.3	Literature Comparison and Limitations of TBR Performance	30
5.	Conclusion and Future prospects	31
References		32
App	endix	vi

List of figures

Figure 1 Illustration of the stepwise degradation of organic matter into biogas (Schnürer, 2018; 1	_
Haq and Kalamdhad, 2022)	2
Figure 2 Process flow diagram illustrating the production of CH ₄ from food waste through	
anaerobic digestion, with hydrogen production from water and acetate production in	a
TBR	. 4
Figure 3 Schematic diagram of the experimental setup, illustrating the flow of digestate and	
substrate between the TBR and the CSTR	7
Figure 4 Flow diagram of the TBR system with gas (70.15% H ₂ /29.85% CO ₂) supply,	
humidification, recirculation loop, pH and temperature control, magnetic stirring and	
gas outflow analysis including H ₂ S removal and flow measurement	10
Figure 5 Schematic of the CSTR with a working volume of 5.4 L. The setup includes heating,	
temperature control, gas sampling with cooling, and an external gas reservoir with	
inductive level sensors.	11
Figure 6 Acetate concentration in TBR 1 over 80 days. Vertical lines indicate media swaps (03.0	14,
22.04, 06.05, and 13.05.25).	14
Figure 7 Acetate concentration in TBR 2 over 22 days. Vertical lines indicate media swaps	
(21.05.25 and 28.05.25).	15
Figure 8 Acetate concentration profiles for TBR 1 1B0 and TBR 2 2B5 over 9 days	15
Figure 9 Development of acetate concentration in TBR 1 (blue triangles) and TBR 2 (red triangle	es)
compared with reference data from the literature: Steger TBR3 (yellow squares),	
Devarapalli (black diamonds), Hiebl CHER II Day 0-35 (green circles), Hiebl CHER	Ι
Day 8-40 (grey circles) and Hiebl CHER I Day 115-155 (purple circles). Media	
exchanges for TBR 2 after 16 leads to a drop in concentration.	16
Figure 10 Acetate production rate in TBR 2 over 21 days. With exchange media at the 9day and	16
days	18
Figure 11 Comparison of volatile fatty acid distribution in TBR 1 1B0 (02.04.25) and TBR 2 2B	5
(28.05.25), displayed as C-mol% and g/L. Each bar pair represents the same sample i	n
two units: C-mol% (left) and concentration in g/L (right). Acetate is shown in orange	,
propionate in grey, isobutyrate in yellow, butyrate in blue, and isovalerate in green.	
Each batch was running in the same time amount of 9days	18
Figure 12 Acid composition in TBR 2 over 21 days, presented in C-mol units. The left Y-axis	
represents the concentrations of propionate (grey), isobutyrate (yellow), butyrate	
(blue), and isovalerate (green). The right Y-axis shows the concentration of acetate	
(orange)	19

Figure 13 Acid composition in TBR 1 over 77 days, showing concentrations of propion	ate (grey),
isobutyrate (yellow), butyrate (blue), isovalerate (green), and acetate (orang	e) in C-mol
units.	19
Figure 14 Gas phase composition in TBR 1 over time. Concentrations of hydrogen (blu	e), CO ₂
(grey), and CH ₄ e (green) are shown	21
Figure 15 Gas composition in TBR 2 over time. The plot shows concentrations of hydro	ogen (blue),
CO ₂ (grey), CH ₄ (green). Additionally on secondary axe is acetate (orange).	21
Figure 16 Gas production rates in a CSTR operated with low pH acetate solution over e	eight weeks.
Shown are RRS (green), RRW (blue), and REA (yellow)	24
Figure 17 Gas production rates in a CSTR with high pH acetate solution over 18 days.	Shown are
RRS (blue) and RRA (orange).	24
Figure 18 CH ₄ production over time in reactors fed with low-pH acetate solution. The g	graph shows
daily CH ₄ production (mL/day) over 8 weeks for RRS (green), RRW (blue),	, and RRA
(orange)	25
Figure 19 CH ₄ production over time in reactors fed with high-pH acetate solution. The	graph
shows daily CH ₄ production (mL/day) over 18 days for RRS (green) and RF	RA
(orange)	25

List of equations:

Equation (1) Acetate into methane and carbon dioxide	5
Equation (2) Hydrogenotrophic methanogenesis, carbon hydroxide reduced by hydrogen	5
Equation (3) Hydrogen and carbon oxide to acetic acid and water	9
Equation (4) Production rate of acetate in TBR	10
Equation (5) Transfer from acetate and water into methane and bicarbonate in CSTR	22
Equation (6) Ideal gas law	22

List of tables

Table 1 TS/VS of the effluent of the biogas plant	. 8
Table 2 Production rates [g/L/day]of acetate from various scientific sources.	17
Table 3 Calculated Gas Production Based on 100 g of TBR 1 pH 5.8-6.3 and TBR 2 pH 8.7-9.0	23

List of appendixes

Appendix table 1 CSTR data for the complet time period	V1
Appendix table 2 TS/VS for all materials	vi
Appendix table 3 Hydraulic retention time of the CSTR	vi
Appendix table 4 TBR1 VFA g/L	vi
Appendix table 5 TBR 2 VFA g/L	vii
Appendix table 6 TBR1 VFA C-mol	viii
Appendix table 7 TBR2 VFA C-mol	ix
Appendix table 8 Gascontent measured with Biogas 5000	X
Appendix table 9 Statistic test gas content	xi
Appendix table 10 TBR1 TCD data	xii
Appendix table 11 TBR2 TCD data	XV

Abbreviations

AD Anaerobic digestion

HRT Hydraulic retention time

VFA Volatile fatty acids

TS Total solids
VS Volatile solids
PtG Power to Gas

HPLC High-performance liquid chromatography

CSTR Continuous stirred tank reactor

TBR Trickle Bed Reactor
GC Gas chromatography
2-BES 2-Bromoethanesulfonate
RRW Reference reactor water
RRS Reference reactor substrate
RRA Reactor reactor acetate

TBR1-Ac TBR 1 acetate-enriched liquid TBR2-Ac TBR 2 acetate-enriched liquid

 H_2S Hydrogen sulphide CO_2 Carbon dioxide

CH₄ Methane

1. Introduction

Europe is currently facing challenges in securing its gas supply and reducing its reliance on fossil fuels. The conflict in Ukraine has put pressure on the price of biofertilizer for agriculture (Vos *et al.*, 2025). One potential solution is to increase domestic biogas production, which could enhance energy security, increase the production of fertilizer, reduce dependence on imports and support climate neutrality.

1.1 Biogas and climate change

Fossil fuel use, and greenhouse gas emissions have disrupted the climate, with six of the nine Planetary Boundaries exceeded by 2025 (Dao and Friot, 2025). In response, the European Union aims for net-zero emissions by 2050 through the European Green Deal (Salvetti *et al.*, 2023; Dupont *et al.*, 2024). Natural gas is expected to play a crucial role in the transition to a lower-carbon economy, acting as a cleaner alternative to coal and providing backup for renewable energy sources (Salehi *et al.*, 2022) Biogas and biomethane have also gained attention as renewable fuels that could reduce greenhouse gas emissions. With appropriate policies in place, the biogas industry could reduce global greenhouse gas emissions by 3.29 to 4.36 gigatons of CO₂ equivalent—around 10 to 13% of total global emissions. (Farghali *et al.*, 2022; Bakkaloglu and Hawkes, 2024).

1.2 Hydrogen

As the transition to sustainable energy technologies accelerates, hydrogen is increasingly seen as essential for storing and delivering large amounts of clean energy. It is expected to play a key role in renewable energy systems, especially in managing the variability of wind and solar power (Ludwig et al., 2015). The widespread use of hydrogen depends on advancements in Power-to-Gas (PtG) technologies, which convert surplus renewable electricity into hydrogen. These technologies are vital for integrating hydrogen into the energy system and realizing its potential as a large-scale, flexible, low-carbon energy solution (Glenk et al., 2023). The primary challenges in the storage and transport of hydrogen arise from its small molecular size and high diffusivity, which can lead to leakage, material degradation, and increased safety risks (Xie *et al.*, 2024). In particular, unintended hydrogen release may result in the formation of flammable mixtures with air, especially in limited or poorly ventilated environments (Davies, Ehrmann and Schwenzfeier-Hellkamp, 2024; Xie *et al.*, 2024).

1.3 Anaerobic digestion

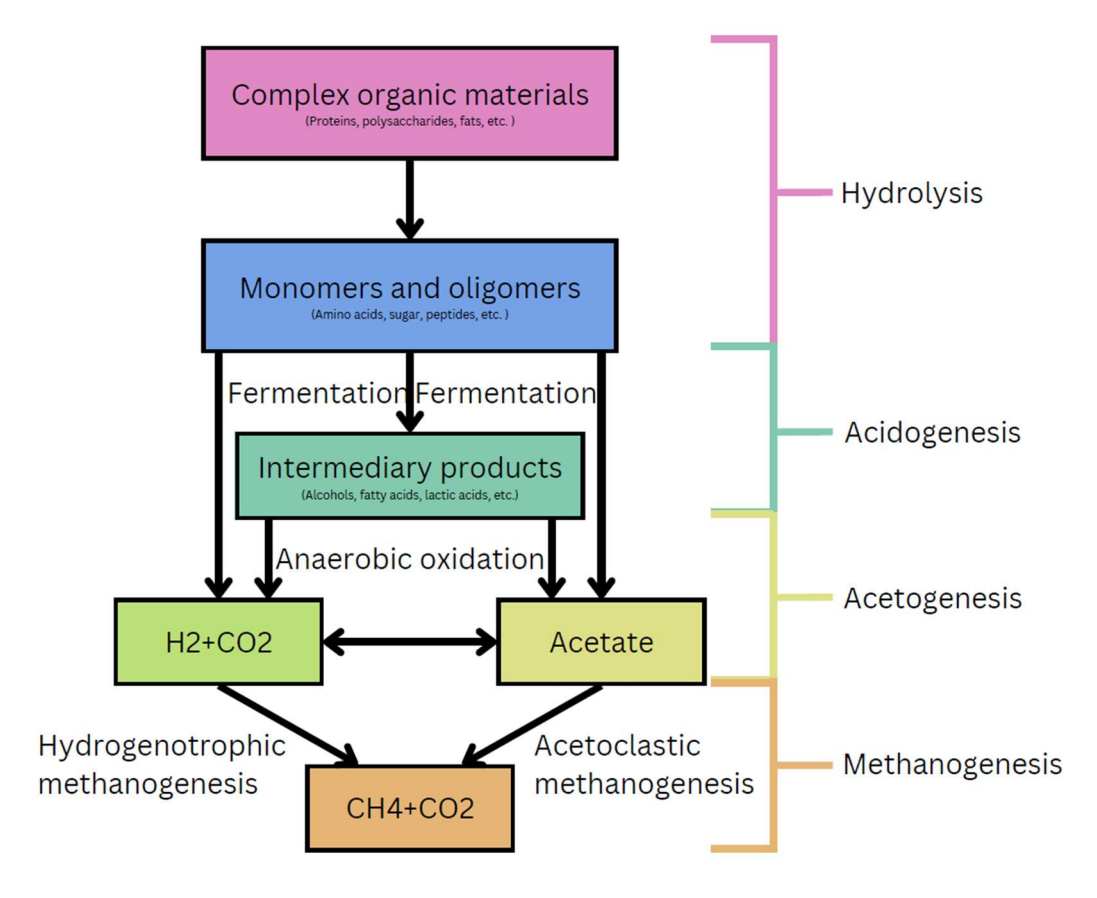


Figure 1 Illustration of the stepwise degradation of organic matter into biogas (Schnürer, 2018; Tg, Haq and Kalamdhad, 2022)

Hydrolysis

During the hydrolysis step in the biogas reactor, complex organic materials are converted into simpler organic compounds, such as amino acids, sugars, fatty acids, and alcohol, using organic waste.

Acidogenesis and Acetogenesis

In the acidogenesis stage, fermentative microorganisms break down monomers and oligomers produced during hydrolysis, such as amino acids, sugars, and peptides. These microorganisms primarily convert these substrates into volatile fatty acids (VFAs) but also generate by-products like alcohols, ammonia, hydrogen sulphide (H₂S), and carbon dioxide (CO₂). Following this stage is acetogenesis, where acetogenic bacteria further decompose the intermediates created during acidogenesis. In this process, compounds such as alcohols and VFAs are transformed into acetate, hydrogen, and CO₂. The specific composition of the products generated during fermentation depends on the environmental conditions and the starting materials used (Schnürer, 2018).

The environmental conditions are:

• **Temperature:** Temperature has a significant impact on microbial activity. With the optimum temperature, the organism grows fast and works more efficiently.

This temperature is strongly linked to the environment from which it originates. The microorganisms are grouped depending on the temperature in psychrophilic (below 20°C), mesophilic (20–50°C), and thermophilic (45–70°C) (Tg, Haq and Kalamdhad, 2022; He *et al.*, 2025).

- **pH:** Like temperatures, a pH value that is too high or too low can disrupt organisms' growth and even lead to cell death. Most bacteria prefer a neutral pH value of 7 to 7.5. During the fermentation process the acid producing bacteria prefer conditions down to pH 5.0 (Schnürer, 2018).
- Toxicity: Certain substances can act as toxicants and interfere with the biogas process. These toxicants can be classified into organic and inorganic types. Organic toxicants include chlorophenols, aliphatic compounds, and long-chain fatty acids, while inorganic toxicants include ammonia, sulphides, and heavy metals. One of the most common and harmful toxicants is H₂S, which diffuses into cells in its undissociated form, denatures proteins and disrupts the microorganism's ability to metabolize (Tg, Haq and Kalamdhad, 2022). 2-Bromoethanesulfonic acid (2-BES) is a specific inhibitor of methanogens that interferes with the enzyme methyl-coenzyme M reductase, which is essential for methane (CH₄) formation (Zinder, Anguish and Cardwell, 1984; Qiu *et al.*, 2023).

Anaerobic Oxidation

During anaerobic oxidation, the products formed during fermentation are broken down into smaller molecules. This process creates a balance between the bacteria that carry out the oxidation and the CH₄ producers. When this balance is optimal, the maximum amount of CH₄ is produced over a longer period of time (Schnürer, 2018). The primary contributor is hydrogen.

Hydrogen in AD

Hydrogen is a critical intermediate in the anaerobic digestion process. It is produced during the fermentation and acetogenesis stages, where microorganisms break down organic matter into simpler compounds such as VFAs, CO₂, and H₂. These products are then utilized by methanogenic archaea to produce CH₄ (Schnürer, 2018).

1.4 Power to gas

The power-to-gas approach involves converting electricity into a gaseous form, allowing for the storage of excess energy. This method is specially suitable for wind and solar energy, as both can be influenced by weather variations (Divya, Gopinath and Merlin Christy, 2015). Storing energy as gas enhances the flexibility of the energy system and enables long-term storage of energy for seasonal use (Divya, Gopinath and Merlin Christy, 2015; Tichler, Bauer and Böhm, 2022). To make power-to-gas technically viable, a number of experiments involving the direct injection of hydrogen into biogas plants have been done. Experiments under both thermophilic and mesophilic conditions were carried out (Bassani *et al.*, 2015; Szuhaj *et al.*, 2016; Cuff *et al.*, 2020; Kim *et al.*, 2021; Löw, 2024).

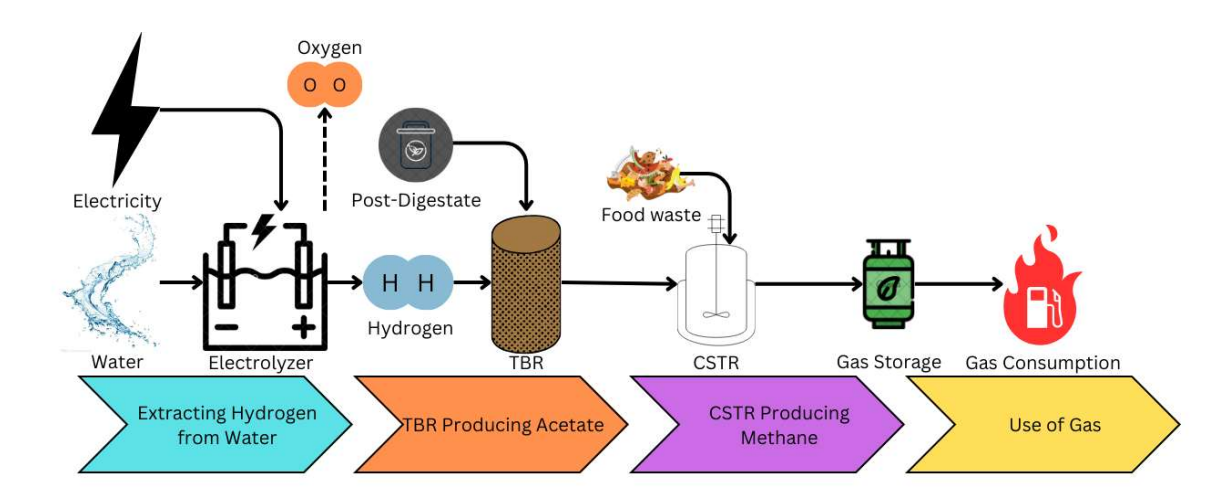


Figure 2 Process flow diagram illustrating the production of CH_4 from food waste through anaerobic digestion, with hydrogen production from water and acetate production in a TBR.

In this master's thesis, a particular implementation of PtG is investigated. Electricity is converted into hydrogen using an electrolyser, as illustrated in Figure 2. For this experiment, those steps are excluded. In a trickle bed reactor (TBR), hydrogen and CO₂ are used to enrich biogas plant substrates with acetate. Acetate offers advantages over hydrogen in terms of storage and safety, as it is less flammable, easier to store under ambient conditions, and compatible with existing liquid fuel infrastructure, reducing costs and complexity (Ni, 2006; Fukuzumi, 2020; Zhang, 2023; Rampai *et al.*, 2024). Methane-producing bacteria then metabolize the acetate in a continuous stirred-tank reactor (CSTR) to generate biogas.

1.5 Relationship between acetogens and methanogens

Acetogens and methanogens coexist in anaerobic systems, often competing for similar substrates. Methanogens assist by using acetate and hydrogen to maintain low hydrogen concentrations, which are necessary for acetogens to function. During the acetogenesis stage of anaerobic fermentation, alcohols and longer-chain volatile fatty acids are primarily metabolized by acetogenic bacteria into acetate, hydrogen, and CO2, typically in syntrophic association with hydrogenotrophic methanogens. Methanogens use these products as substrates in the methanogenesis, which produces CO₂ and CH₄ (Amani, Nosrati and Sreekrishnan, 2010; Sikora et al., 2017). Hydrogenotrophic methanogenesis represents an alternative pathway of CH₄ production that bypasses acetate. In this process, methanogens reduce CO₂ by using hydrogen as the electron donor, producing CH₄ as the end product. The continuous removal of hydrogen by these microorganisms lowers the hydrogen partial pressure, which is necessary for the oxidation of substrates such as propionate and butyrate by syntrophic bacteria. This acetate-independent pathway is favoured under ammonia stress or when acetolactic methanogenesis is suppressed, and can be stimulated by direct hydrogen addition (Luo et al., 2012; Schnürer, 2018). If methanogenesis is inhibited, this balance is disrupted, leading to the accumulation of acetate (Dyksma, Jansen and Gallert, 2020). CH₄ production in the CSTR could proceed via two primary pathways:

First, through acetolactic methanogenesis, where acetate produced by microorganisms was directly converted into methane and carbon dioxide:

$$CH_3COOH \to CH_4 + CO_2 \tag{1}$$

Alternatively, methane could form through hydrogenotrophic methanogenesis, in which carbon dioxide is reduced by hydrogen:

$$4H_2 + CO_2 \to CH_4 + 2H_2O \tag{2}$$

(Kern *et al.*, 2016; Bajpai, 2017; Schnürer, 2018; Dyksma, Jansen and Gallert, 2020; Zhu *et al.*, 2020; Löw, 2024)

1.5.1 Promoting acetate formation over methanogenesis

2-BES inhibits the methanogenic archaea's metabolic pathways, which causes acetate to accumulate up as a metabolic product. (Zinder, Anguish and Cardwell, 1984; Qiu *et al.*, 2023). While preventing hydrogenotrophic methanogenesis and syntrophic acetate oxidation, high pH levels promote acetate production during glucose fermentation. (Cui, Luo and Liu, 2023). Ammonia stress can interrupt acetolactic methanogenesis and promote syntrophic acetate oxidation (Kato, 2014). Acetate formation is influenced by other environmental factors that restrict hydrogenotrophic methanogens, such as pH, temperature, or competing processes like nitrate reduction. (Klueber and Conrad, 1998; Xu *et al.*, 2015; Fu *et al.*, 2019).

1.6 Aim and Research Question

This Master's thesis aims to explore the transfer of electrical energy to biogas through the use of hydrogen, with a focus on increasing the efficiency of the power cycle. The thesis is divided into two main parts.

The first part investigates the production of acetate in a TBR. In this section, pH and temperature is continuously regulated, and both gas and liquid analyses are performed to visualize the production of organic acids such as acetate, lactate, propionate, butyrate, valerate, and caproate. The goal is to maximize the production rate of VFAs, with a particular focus on acetate.

In the second part, the use of enriched acetate in a CSTR is examined, and the reactor's performance is contrasted with reference reactors. This section primarily focuses on CH₄ production and upgrading, emphasizing its possible industrial uses. The biogas plant in Linköping intend to use that for the effluent of the post digester.

2. Material and Methods

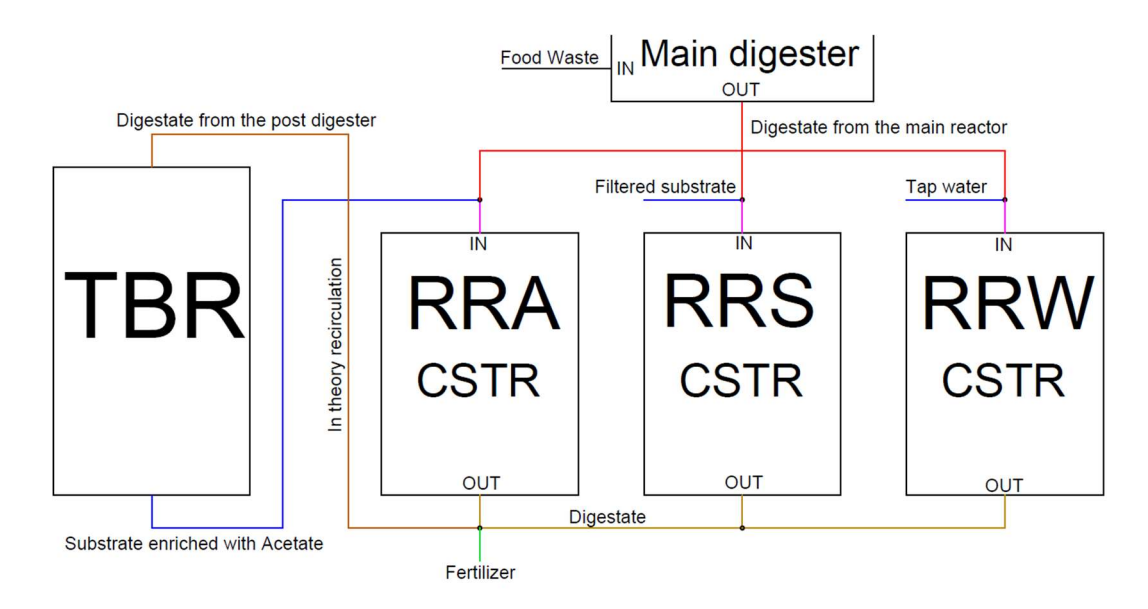


Figure 3 Schematic diagram of the experimental setup, illustrating the flow of digestate and substrate between the TBR and the CSTR.

In this Master's thesis, five reactors were used: two TBRs for the production of acetate and three CSTR for the production of CH₄.

In the process setup visible in figure 3, the main digester effluent was used to feed three CSTRs, which served as the primary methane-producing units. Each CSTR received the main reactor digestate either supplemented with acetate-enriched liquid from the TBR or with one of the two reference substance. The effluent from the CSTRs could be in theory used as fertilizer and to feed the TBRs. Instead of this in theory effluent of CSTR approach, filtered post-digester effluent was directly used and not recycled. In the TBRs, the digestate was biologically enriched with acetate through conversion of hydrogen and CO₂. The resulting acetate-rich liquid was then recirculated into the CSTRs to assess its effect on biogas production.

Two identical TBRs were operated at different pH ranges—one at pH 5.8–6.3 and the other at pH 8.7–9.0. The TBR samples were collected on working days for analysis by gas chromatography (GC) and high-performance liquid chromatography (HPLC). A control unit was installed in the TBR to continuously monitor the concentrations of hydrogen and CO₂.

The inoculum for both the CSTR and TBR was provided by the local biogas producer Uppsala Vatten. The facility primarily receives organic waste from households, large-scale kitchens, and similar sources. A smaller amount comes from industries such as slaughter-houses, the food industry, and grease traps ('Uppsala vattens biogasanläggning', 2021). It consisted of the effluent from the main reactor and the effluent from the post-digester. As

shown in Figure 3, the post-digester effluent is used in the TBR to be enriched with acetate. The idea is to use the enriched substrate to circulate it into the CSTR, where it is used for gas production. Since the post-digester is more stable, the industry in Linköping intends to apply this process only in the post-digester.

Table 1 TS/VS of the effluent of the biogas plant

Description	TS [%]	VS [%]	Stdev
Effluent post digestate	3.60	2.45	0.41
Digestate main reactor 26.02.25	4.02	2.82	0.26
Filtered substrate	1.98	1.32	0.22
Digestate main reactor 21.05.25	4.65	3.24	0.32

The first load of the main reactor had an average TS of 4.02% (see Table 1), with the average VS calculated from triplicates and a standard deviation of 0.26%. The Effluent post-digestate, showed an average TS of 3.60% and a VS of 2.82%, based on triplicate samples, with a standard deviation of 0.41%. Duplicate analysis of the filtered substrate yielded an average TS content of 1.98%, with VS averaging 1.32% and a standard deviation of 0.22%. For the digestate from the new load of the main reactor, the average TS content was measured at 4.65%, while the VS content reached 3.24%, with a standard deviation of 0.32% based on duplicate samples.

Each of the three CSTR was started using inoculum from the effluent of the main reactor, and allowed to run in total for 5 Hydraulic Retention Times (HRTs) in order to establish stable biogas processes. For the experimental period, the reactors were fed on weekdays with 304.4 g of base substrate (post-digestate from the main reactor), and 100 g of additional material: tap water for the water control reactor (RRW), additional filtered post-digestate for the control reactor (RRS), and acetate-enriched TBR effluent for the experimental reactor (RRA). On the 21.05.25 the base substrate was switched to the new digestate main reactor 21.05.25.

The substrate for the TBR 1 was prepared with a pH adjusted to 6 for suppressing the CH₄ production. This adjustment was achieved using 200mL phosphoric acid in the first batch and 30mL hydrochloric acid in all subsequent ones. The substrate was derived from the effluent of the post-digester, first centrifuged and then filtered down to 0.01 mm. In the first batch, 2-BES was added to inhibit methanogenesis, along with a culture of *Moorella thermoacetica* to enhance acetate production. To minimize foam formation during the process, polypropylene glycol 2000 was used as an antifoaming agent.

Similar to the liquid of TBR 1 the substrate in TBR 2 was centrifuged and filtered. The pH was slightly raised with 15mL sodium hydroxide for a batch of 1800mL. No add-ons like 2-BES, cultures or Antifoam were used.

2.1 Design and Function of the TBR

The TBR stimulates the conversion of hydrogen and CO₂ into acetic acid, a process driven by acetogenic bacteria that generate acetate. This is shown in the equation (1). The reactor utilises an improved gas-liquid mass transfer so that the cells remain in the system by forming a biofilm on the carriers (Steger et al., 2022). The carrier liquid was continuously recirculated, and acetate concentration was monitored daily. Process was stopped once acetate accumulation plateaued or no further increase was observed, or the liquid was subsequently required for use in the CSTR.

Hydrogen reacts with carbon dioxide to form acetic acid and water:

$$4H_2 + 2CO_2 \rightarrow CH_3COOH + 2H_2O$$
 (1)
(Schnürer, 2018; Löw, 2024)

Before the initial start-up, the system was rinsed with tap water until visibly clean. No further cleaning was performed between batches. The filtered effluent from the post digester was pH-adjusted to ~6 and ~9 for TBR 1 and TBR 2 and then stored in a 2 L glass reservoir. Liquid from the reservoir was pumped into the reactor and a defined Volume of 22mL was recirculated every 10 minutes using a peristaltic pump, which ensured consistent flow and the formation of a stable liquid film over the carrier material within the TBR. The carrier material used in the TBR was Filtralite® Nature NC 2–10mm, a porous medium produced from expanded clay (Saltnes, Eikebrokk and Ødegaard, 2002).

During the experiment, a continuous supply of hydrogen and CO₂ was maintained to prevent under pressure and minimize the risk of oxygen intrusion. In the gas mixture, CO₂ served as a key reactant in acetate production and influenced pH through dissolution.(Siegel and Ollis, 1984; Yu and Munasinghe, 2018). To stabilize the pH within the feed reservoir, a pH control unit with a dosing pump was used. Since acid formation during acetate production can lower the pH, sodium hydroxide (NaOH) was added as a pH regulator. Temperature regulation was accomplished using an internal temperature sensor in the liquid medium, connected to an external heating element. The temperature was adjusted to 52°C. After the second batch, the heating for the storage was turned off. The liquid substrate in the reservoir was continuously stirred at a speed of 300 rpm using a magnetic stirrer. Gas flow into the reactor was regulated by a Mass Flow Controller (MFC) to maintain a consistent feed and prevent over-delivery. The gas flow was manually regulated according to the bacteria's consumption as judged by the measured gas outflow. Additional gas was supplied during times of high consumption. The gas mixture that entered the system was humidified. Inside the reactor, the gas passed through a packed bed of Filtralite Nature NC 2-10, which provided attachment surfaces for the microbial community and enhanced mass transfer.

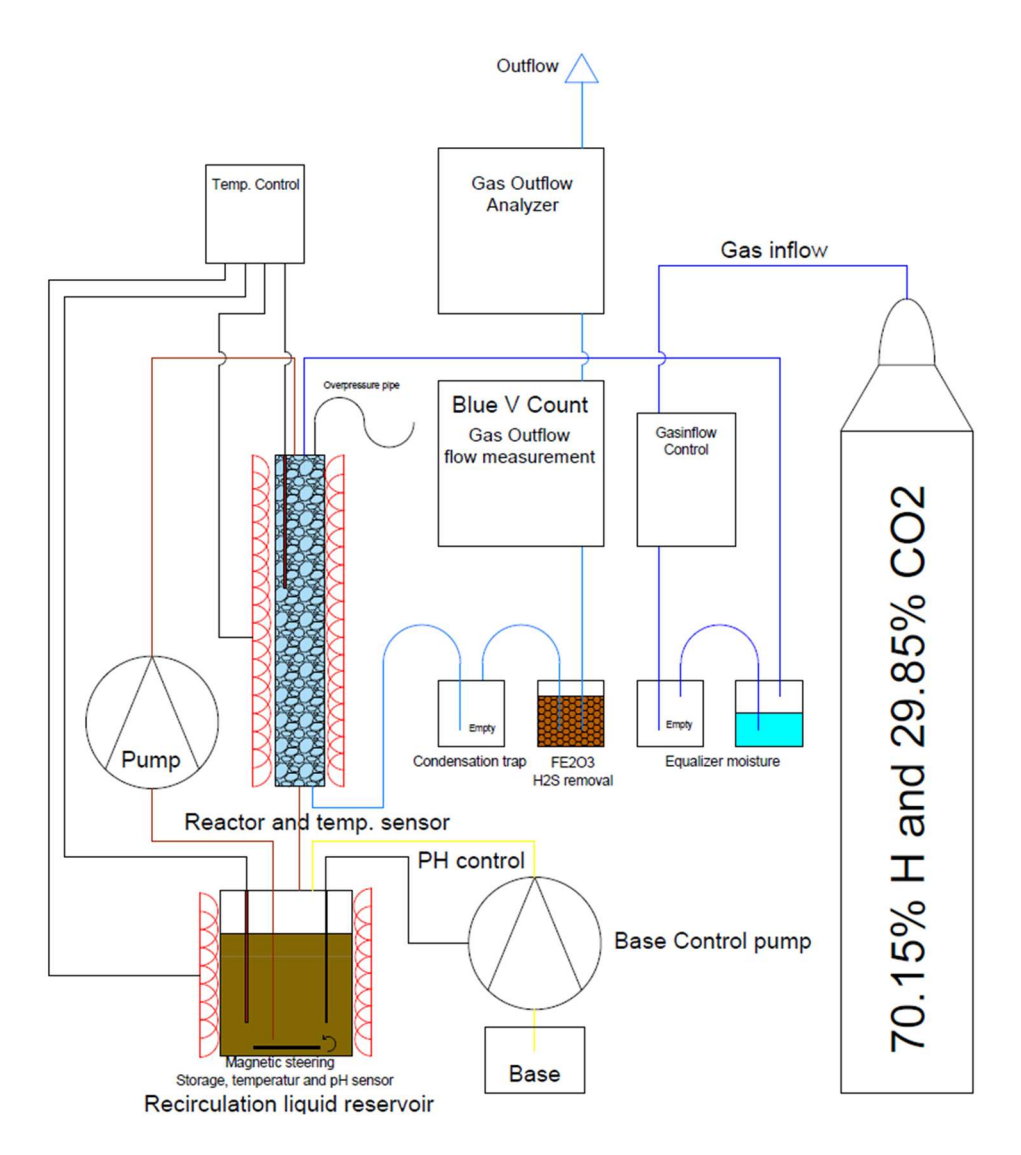


Figure 4 Flow diagram of the TBR system with gas $(70.15\% H_2/29.85\% CO_2)$ supply, humidification, recirculation loop, pH and temperature control, magnetic stirring and gas outflow analysis including H_2S removal and flow measurement.

To prevent gas accumulation and pressure fluctuations caused by gas bubbles, a water-filled pressure relief pipe was installed. This allowed excess gas to escape safely and prevented overpressure. Condensation traps were used to remove water vapour from the gas stream, and H₂S were removed using a Fe₂O₃-based filter. Volumetric gas flow was continuously monitored using a gas flow meter, while gas composition was determined using a calibrated gas analyser. Samples for GC and HPLC were drawn from the liquid reservoir using syringes.

Calculations of the production rate for the TBR

$$Pr = \frac{C_2 - C_1}{t_2 - t_1} \tag{4}$$

Pr = Production rate

 $C_1, C_2 = \text{Concentrations}$ at the time t_1 and $t_2 [g/L]$

 t_1,t_2 = Time [days]

The production rate of the acetate in the TBR was calculated by the change of concentration of the TBR reactor over time, comparable to the literature (Steger *et al.*, 2022; Hiebl *et al.*, 2025).

2.2 CSTR Setup and Operation

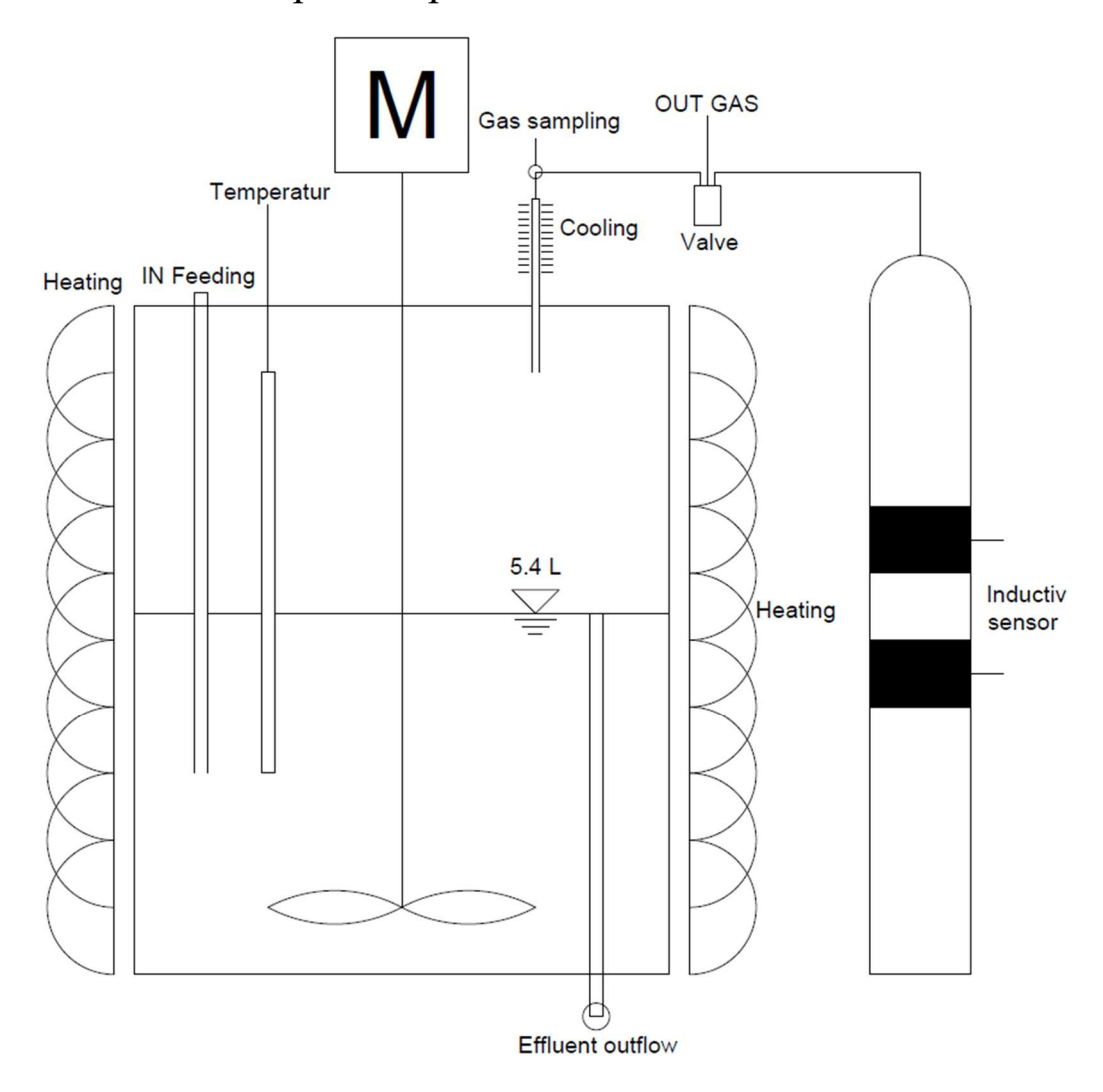


Figure 5 Schematic of the CSTR with a working volume of 5.4 L. The setup includes heating, temperature control, gas sampling with cooling, and an external gas reservoir with inductive level sensors.

In the CSTR, microorganisms were cultivated under controlled conditions, replicating the environment of a biogas plant's secondary digester at 46°C. This reactor served as a scaled-down model of a full-scale biogas facility. All three reactors had a settling-in period of about 3 weeks until the gas production was in similar ranges. The reactor's contents were mixed continuously by a motor-driven impeller operating at 90 rpm. The working volume of 5.4 litres was maintained by an adjustment pipe that controlled the liquid level. Biogas produced in the reactor was first cooled to ambient temperature before being measured continuously using inductive sensors, allowing for ongoing monitoring of gas flow. In

addition to gas flow measurement, weekly samples were taken for FOS/TAC analysis and microbiological studies. The gas composition was analysed twice per week using a Biogas 5000 device. When the Biogas 5000 was unavailable, CO₂ levels were instead monitored using a Einhorn's saccharometer.

Hvdraulic retention time:

The hydraulic retention time (HRT) for the 5.4L CSTR was initially set at 23 days to match the conditions of the biogas plant in Uppsala. This setup was maintained until the gas production of the three reactors reached a comparable level. Once the experiment began, the HRT was reduced by five days, because of the addons with the base food. The hydraulic retention time remains the same for the three reactors in the experiment.

2.3 Process Monitoring and Analysis

2.3.1 Biogas 5000

For on-site analysis of biogas composition, the BIOGAS 5000 portable gas analyser from the company "Q.E.D. Environmental Systems Ltd." was used. This instrument is designed for monitoring anaerobic digestion. It detects gas components, including CH₄, CO₂, oxygen, H₂S and other gases. The analyser features an electrochemical and infrared sensor array, providing a CH₄ measurement range of 0–100% with an accuracy of $\pm 0.5\%$ within the 0–70% range; similar precision is available for CO₂ measurement (Geotech, 2015).

2.3.2 Gas chromatography

1mL gas samples were taken in triplicate using gas-tight syringes. The collected gas was transferred over a membrane into sealed glass vials with a volume of 22mL. Samples from the TBRs were taken daily, while CSTR samples were collected every two to three weeks.

The gas composition was analysed using a PerkinElmer Clarus 590 gas chromatograph (PerkinElmer, USA) equipped with a TurboMatrix 110 headspace autosampler. Argon was used as the carrier gas under constant flow conditions. Separation of gas components was achieved using two columns in series: a 7' HayeSep N (60/80 mesh) and a 9' Molecular Sieve 13X (45/60 mesh). CH₄ was detected using a flame ionization detector, while CO₂, hydrogen, and nitrogen were measured using a thermal conductivity detector (PerkinElmer, 2017).

2.3.3 FOS/TAC

Process stability was monitored using the FOS/TAC method according to Nordmann (1977), which provides a practical estimate of the relationship between volatile organic acids (FOS) and buffer capacity (TAC) in anaerobic digestion (Lili *et al.*, 2011). A 5 mL of digester effluent was titrated with 0.1 N sulfuric acid (H₂SO₄) using an automatic titrator. The titration was performed in two stages: first, up to pH 5.0 to calculate TAC, which was expressed in mg/L CaCO₃; and second, from pH 5.0 to 4.4 to compute FOS, which was expressed in mg/L as acetic acid (CH₃COOH) (Hach, 2025). While a FOS/TAC ratio above 0.4 suggested the possibility of acidification from the formation of volatile fatty acids, a ratio below 0.3 can be considered stable digestion. (Lili *et al.*, 2011).

2.3.4 High-performance liquid chromatography

For the analysis of VFAs, 700 μ L of reactor contents was mixed with 70 μ L of 5 M sulfuric acid. The samples were then frozen and stored until analysis. Before HPLC measurement, frozen samples were centrifuged at 11,000rpm for 15 minutes. To remove all remaining solids, the resultant supernatant was passed through a 0.2 μ m syringe filter.

Based on the efficiency that a compound retains in a chromatographic column, HPLC separates and measures the compounds in a liquid sample. A Shimadzu 2050 Series HPLC system fitted with an iron exclusion column (Rezex ROA Organic Acids H^+ , 300×7.80 mm) was used to perform chromatographic separation. (Phenomenex, 2025). Under isocratic conditions, the mobile phase, which contained 5 mM sulfuric acid, flowed at a rate of 0.6 mL/min. Since carboxylic acids absorb well in this range, the detection was carried out with a UV detector set to 210 nm (Fujimura and Matsumoto, 2021).

3. Result

3.1 TBR

3.1.1 Comparison between TBR1 and TBR2

A continuous measurement of acetate concentrations, including all sampling points collected throughout the entire experimental period, is shown for TBR 1 and TBR 2 in Figures 6 and 7. Figure 8 presents a direct comparison of the best-performing run from each reactor.

Continous TBR 1 curve 2 1.8 1.6 Acetate [g/L] 1.4 1.2 0.8 0.6 0.6 0.4 0.2 0 0 10 20 30 40 50 60 70 80 90 Time [days]

Figure 6 Acetate concentration in TBR 1 over 80 days. Vertical lines indicate media swaps (03.04, 22.04, 06.05, and 13.05.25).

In TBR 1 (Figure 6), the acetate concentration reached a maximum of 1.5 g/L during the initial 15 days of operation. Each media exchange, indicated by vertical lines, was followed by a pronounced decrease in acetate levels. In the subsequent course of the experiment, acetate concentrations remained low and stabilized below 0.4 g/L after the final media exchange. Over the full 80-day period, a general downward trend in acetate production was observed.

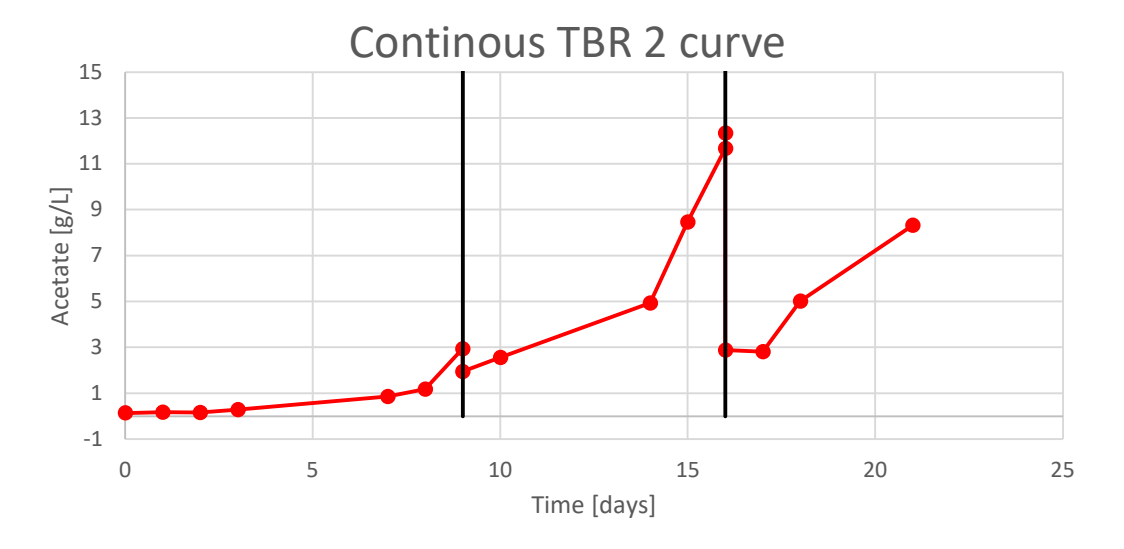


Figure 7 Acetate concentration in TBR 2 over 22 days. Vertical lines indicate media swaps (21.05.25 and 28.05.25).

In contrast, TBR 2 achieved noticeably higher acetate concentrations (Figure 7). After a short lag phase, acetate levels increased sharply after each media exchange and peaked at approximately 12.4 g/L within 22 days. Unlike TBR 1, no significant decline in acetate concentration was detected following the media swaps in TBR 2, indicating a more stable and efficient production process.

Acetate Curve TBR 1 1B0 and TBR 2 2B5

14 12 10 8

Acetate [g/L] 6 4 2 0 6 8 10 0 12 Time [days] **-**1B0 **─** 2B5

Figure 8 Acetate concentration profiles for TBR 1 1B0 and TBR 2 2B5 over 9 days.

This difference is further illustrated in Figure 8, which shows the acetate concentration curves for both reactors over nine days. In Figure 6, curve TBR 1 1B0 represents data from day 7 to day 16, while in Figure 7, curve TBR 2 2B5 corresponds to the period from day 9 to day 16. While TBR 1 showed linear low acetate levels, TBR 2 exhibited a rapid increase on day 5 to 7, reaching a maximum of approximately 12.4 g/L by day 8.

3.1.2 Comparison with literature

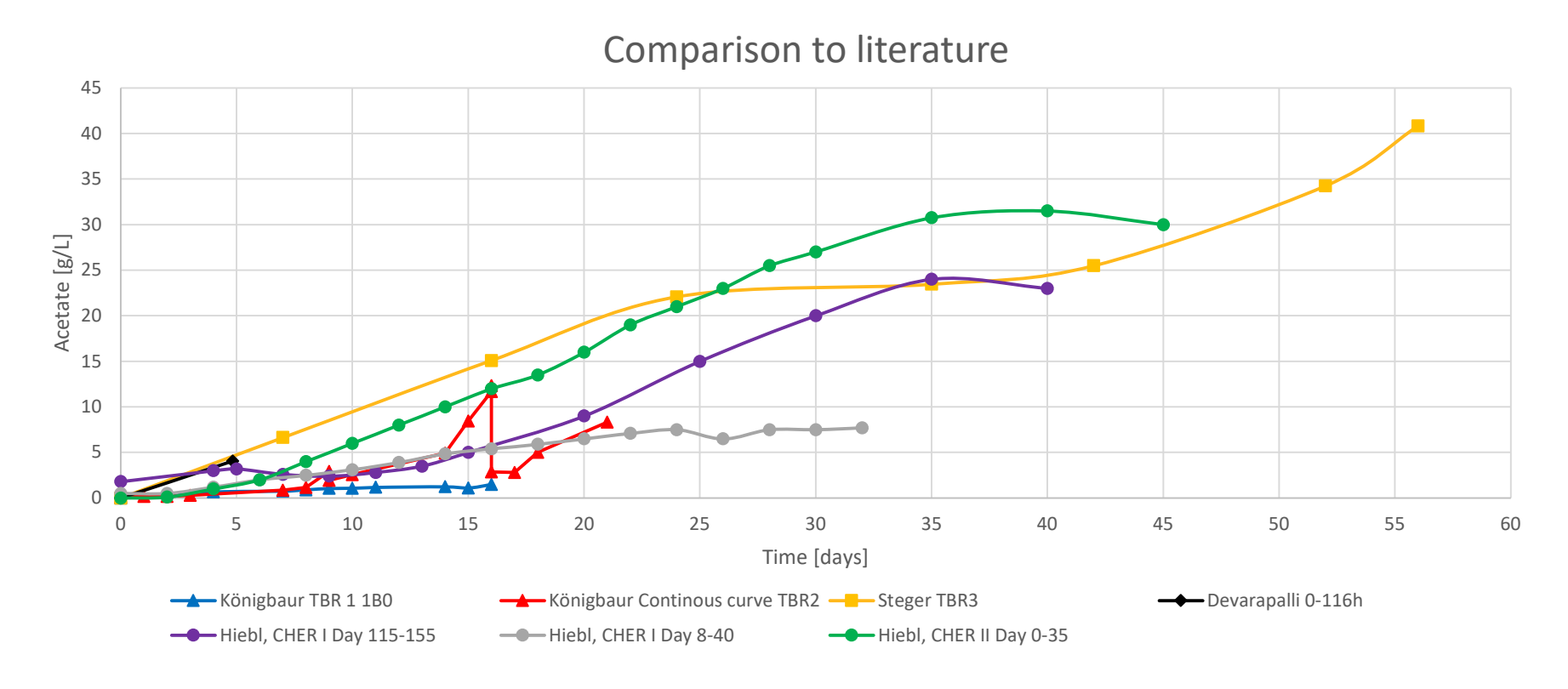


Figure 9 Development of acetate concentration in TBR 1 (blue triangles) and TBR 2 (red triangles) compared with reference data from the literature: Steger TBR3 (yellow squares), Devarapalli (black diamonds), Hiebl CHER II Day 0–35 (green circles), Hiebl CHER I Day 8–40 (grey circles) and Hiebl CHER I Day 115–155 (purple circles). Media exchanges for TBR 2 after 16 leads to a drop in concentration.

For the comparison with literature, only studies employing similar reactor designs and operational conditions were considered. The main parameters taken into account included pH, reactor configuration (TBR), substrate, and gas composition (hydrogen and CO₂ flushing). Production rates and acetate concentrations from this study were compared with published results from Devarapalli et al. (2016), Steger et al. (2022) and Hiebl et al. (2025).

Figure 9 shows the development of acetate concentrations in TBR 1 and TBR 2, compared with reference data from Devarapalli et al. (2016), Steger et al. (2022), and Hiebl et al. (2025). TBR 2 (red triangles) experienced a rapid increase in acetate during the first 20 days, peaking at about 12.4 g/L before stabilizing. In contrast, TBR1 (blue triangles) maintained low concentrations, below 2 g/L. Different reference systems showed distinct patterns of acetate accumulation. Steger's TBR3 (yellow squares) reached over 40 g/L after 55 days, while Hiebl's CHER II (green circles) attained about 30 g/L by day 35. Hiebl's CHER I showed stabilizing trends at 8 g/L and eventually reached 25 g/L, while Devarapalli's system (black diamonds) reach above 5 g/L after 5 days. Notably, TBR 2 underwent a media exchange after day 16, leading to a temporary drop in acetate concentration.

Table 2 Production rates [g/L/day] of acetate from various scientific sources.

Source	Production Rate *[g/L/day]
Devarapalli	2.34
Steger TBR 3	1.12
Hiebl Cher I	0.94
Hiebl Cher II	0.91
Königbaur TBR 1	0.38
Königbaur TBR 2	3.53

Table 2 lists the acetate production rates measured in this study and reported in the literature. Devarapalli et al. achieved a rate of 2.34 g/L/day, Steger TBR 3 reached 1.12 g/L/day, Hiebl-Cher I 0.94g/L/day, and Hiebl-Cher II 0.91 g/L/day. In the present master thesis, TBR 1 yielded 0.38 g/L/day, while TBR 2 achieved 3.53 g/L/day.

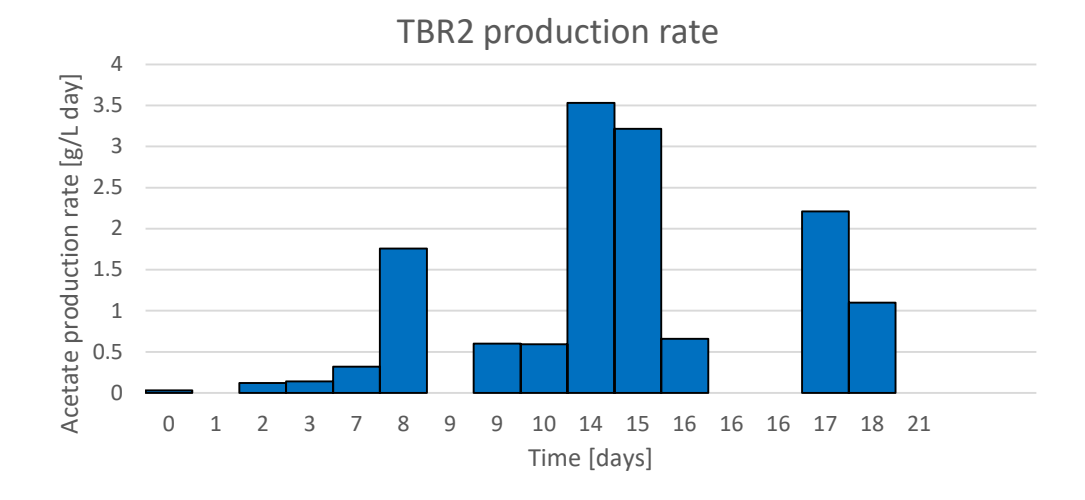


Figure 10 Acetate production rate in TBR 2 over 21 days. With exchange media at the 9day and 16 days.

The production rate increased sharply after day 9, reaching a maximum of 3.53 g/L·day between days 14 and 15.

3.1.3 Acid composition in TBR

The composition of volatile fatty acids in both reactors was analysed during the experimental period with HPLC. Other acids like capoarate and lactate were not present in both reactors. Acid concentrations in all diagrams are presented as C-mol, ensuring carbon-based comparability.

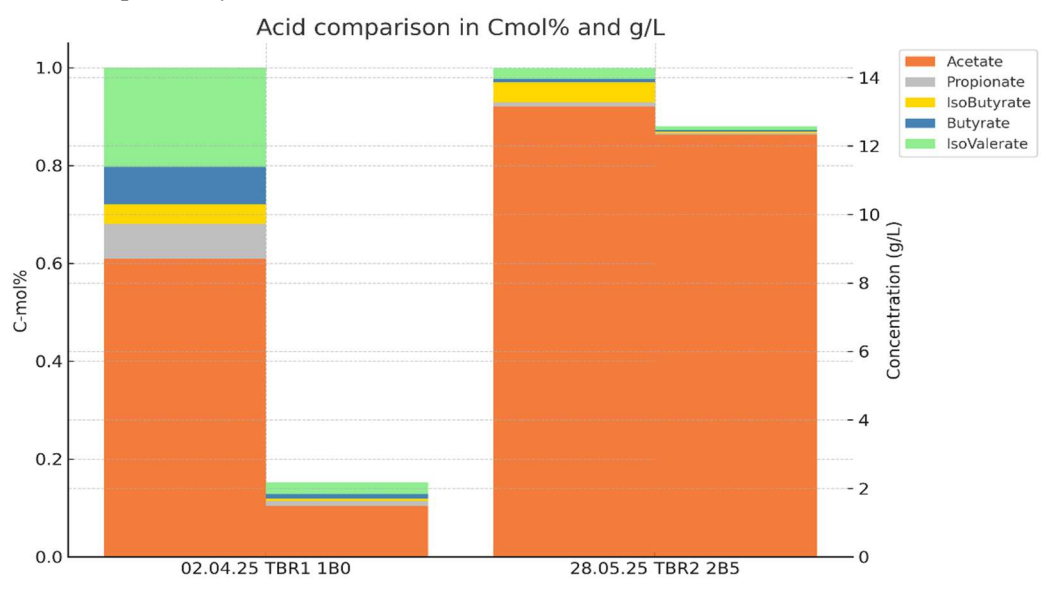


Figure 11 Comparison of volatile fatty acid distribution in TBR 1 1B0 (02.04.25) and TBR 2 2B5 (28.05.25), displayed as C-mol% and g/L. Each bar pair represents the same sample in two units: C-mol% (left) and concentration in g/L (right). Acetate is shown in orange, propionate in grey, isobutyrate in yellow, butyrate in blue, and isovalerate in green. Each batch was running in the same time amount of 9days.

As shown in Figure 11, acetate was the predominant acid in both reactors, with higher levels observed in TBR 2. Minor amounts of propionate, isobutyrate, butyrate, and isovalerate were detected, with TBR 1 showing a broader distribution of by-products.

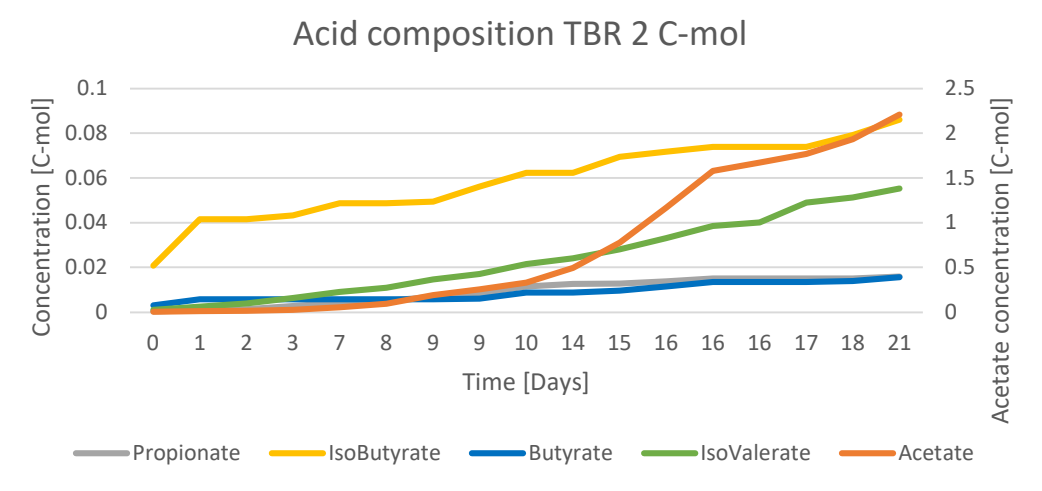


Figure 12 Acid composition in TBR 2 over 21 days, presented in C-mol units. The left Y-axis represents the concentrations of propionate (grey), isobutyrate (yellow), butyrate (blue), and isovalerate (green). The right Y-axis shows the concentration of acetate (orange).

The Figure 12 displays the acid composition in TBR 2 over a period of 21 days. Acetate concentrations increased steadily and remained the dominant component. Propionate, isobutyrate, butyrate, and isovalerate were present in minor amounts and showed only moderate changes during the observation period.

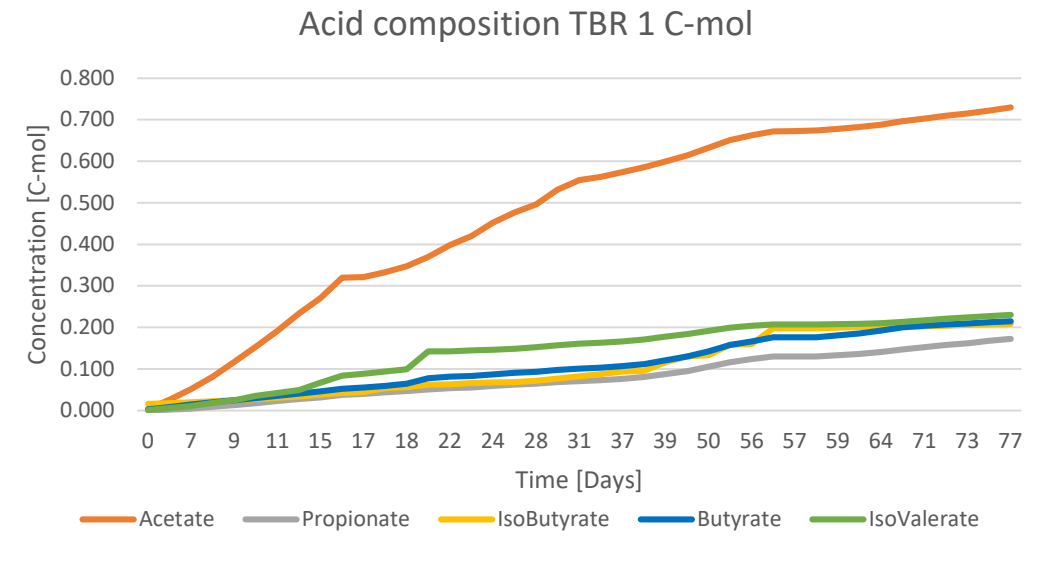


Figure 13 Acid composition in TBR 1 over 77 days, showing concentrations of propionate (grey), isobutyrate (yellow), butyrate (blue), isovalerate (green), and acetate (orange) in C-mol units.

Figure 13 illustrates the acid profile in TBR 1 over 77 days. Acetate remained the major acid, but the relative amounts of isovalerate, butyrate, and isobutyrate were higher compared to TBR 2. Propionate was detected in low concentrations. No caproate or lactate was found in either reactor.

3.1.4 Process Disturbances and Contamination

Temperature failures

A self-regulating temperature control unit caused recurring temperature fluctuations within the TBR 1 reactor system. In response, the control unit was temporarily deactivated and reprogrammed, stabilising the temperature for a limited period. Over time, the amplitude of the fluctuations gradually increased again. The reprogramming procedure required the system temperature to be briefly raised above 60°C.

On the night of 24 to 25 April, a malfunction of the temperature control system occurred in TBR 1. As a result, the storage vessel overheated while the temperature in the glass cylinder dropped to ambient levels. This event led to abrupt shifts in acetate production, indicating a disturbance of microbial activity within the reactor. After this event, the storage heating for both reactors detached.

Contamination

Probably contamination occurred at the backflow of the indicator solution phenolsulfonphthalein (C₁₉H₁₄O₅S) through the overpressure line during an under-pressure event in TBR 1 in mid of April.

3.1.5 Gas Compositions

The gas composition in TBR 1 and TBR 2 was monitored with GC.

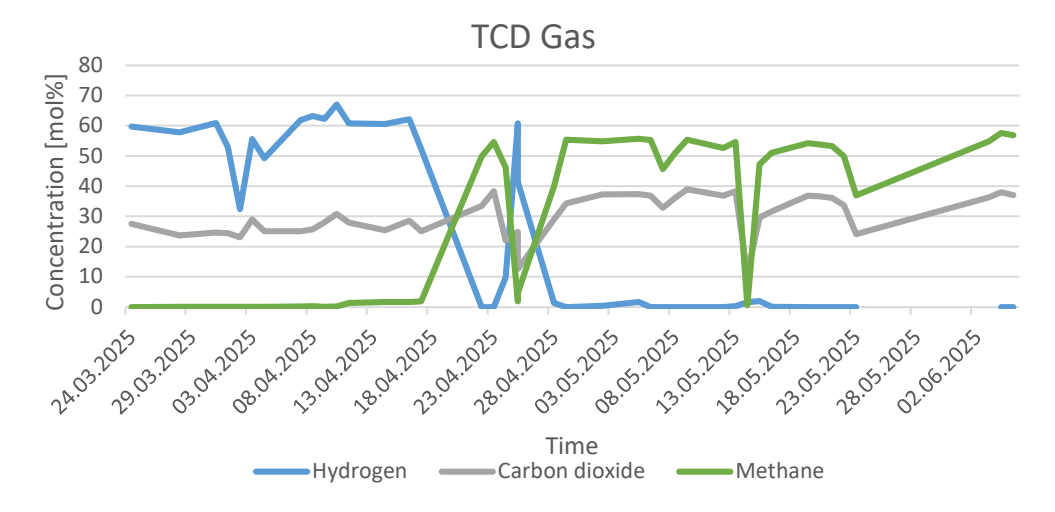


Figure 14 Gas phase composition in TBR 1 over time. Concentrations of hydrogen (blue), CO_2 (grey), and CH_4e (green) are shown.

In the figure 14 the hydrogen levels were initially high and decreased sharply at several time points, while methane concentrations increased correspondingly. CO₂ remained relatively stable throughout the experiment.

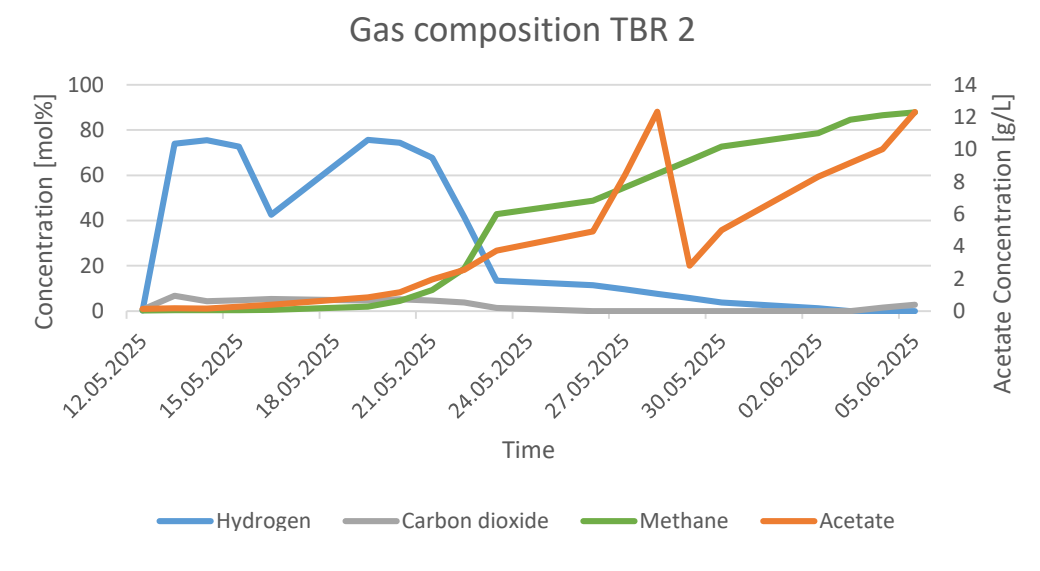


Figure 15 Gas composition in TBR 2 over time. The plot shows concentrations of hydrogen (blue), CO_2 (grey), CH_4 (green). Additionally on secondary axe is acetate (orange).

As shown in Figure 15, hydrogen and CO₂ were initially present at high concentrations in the gas phase. Both gases declined after 21.05.2025, which coincided with an increase in methane production. Methane concentrations increased steadily over time, peaking at the end. Acetate concentrations, shown on the secondary axis, also increased during this period, with a marked rise observed after the drop in hydrogen and CO₂.

3.2 CSTR

3.2.1 Calculation gas production

Based on the stoichiometric the equation is:

$$CH_3COO^- + H_2O \to CH_4 + HCO_3^-$$
 (5)

acetate and water are converted into methane and bicarbonate under anaerobic conditions. The theoretical methane yield can be estimated using the ideal gas law:

$$p * V = n * R * T \tag{6}$$

p = pressure of the gas [Pa]

 $V = \text{volume occupied by the gas } [m^3]$

n = amount of substance (moles of gas) [mol]

R = universal gas constant (8.314 J·mol⁻¹·K⁻¹)

T = absolute temperature [K]

Assuming standard pressure conditions 1013.25 hPa and a temperature of 46 °C, 1 gram of acetate corresponds to the production of approximately 0.443 L of methane. This conversion factor was used to calculate the impact of acetate addition on methane production in the CSTR.

Based on experience, a 10% increase in methane volume would be clearly distinguishable from baseline (S. Isaksson, pers. comm.). Under the assumption that the daily gas production of the CSTR is around 800 mL, and that the methane content is 60%, the resulting methane production is approximately 480 mL per day. A 10% increase in methane production correspond to 528 mL of methane, leading to a gas production of 880 mL per day. Using the conversion factor (1 g acetate = 0.443 L CH₄), the amount of acetate required to generate additional 48 mL of methane is:

$$48 \text{ mL} / 443 \text{ mL/g} \approx 0.108 \text{ g of acetate}$$

This amount represents the lowest acetate dosage required to produce a detectable rise in methane production. Higher dosages of acetate are expected to yield larger effects. During the first acetate dosing experiment, an acetate concentration of 1.485 g/L was measured. To provide 0.108 g of acetate from this solution, a total volume of:

10% higher gas production: $108.4g / 1.485 g/L \approx 73 mL$

of TBRs liquid would be needed. Since the TBRs cannot produce an exact acetate content, and the HRT should remain constant, the liquid was limited to 100 g. Due to the fluid's low viscosity and near water-like density, it is assumed for simplification that 100 grams of acetate solution are equivalent to 100 millilitres.

Table 3 Calculated Gas Production Based on 100 g of TBR 1 pH 5.8-6.3 and TBR 2 pH 8.7-9.0

	Acetate [g/L]	Gasproduction [mL]	Increase [%]
1B0	1.49	65.79	13.71
1B1	0.71	31.63	6.59
1B2	0.43	18.91	3.94
1B3	0.29	12.93	2.69
1B6	0.40	17.54	3.65
2B4	2.93	129.62	27.00
2B5	12.33	546.40	113.83
2B7	12.31	545.11	113.56

The theoretical methane production based on acetate concentrations in different TBR batches, based on 100 g of batch liquid, is summarized in table 3. A conversion factor of 1 g acetate = 0.443 L CH₄ is used in the calculation. With an acetate concentration of 1.49 g/L, the estimated methane yield in Batch 0 (1B0) was 65.79 mL, indicating a 13.7% increase. With 0.71 g/L acetate, Batch 1 (1B1) produced 31.63 mL of methane (6.6% increase). Methane productions of 18.91 mL, 12.93 mL, and 0.40 corresponding to lower concentrations in Batches 2 (1B2: 0.43 g/L), 3 (1B3: 0.29 g/L), and 6 (1B6: 0.4 g/L) increased by 3.94%, 2.69%, and 3.65%, respectively. Batch 4 (2B4) achieved 2.93 g/L acetate for TBR 2, resulting in 129.62 mL methane and a 27.0% increase. With 12.33 g/L acetate, Batch 5 (2B5) had the highest values, resulting in a calculated methane production of 546.40 mL and an increase of 113.83%. Results from Batch 7 (2B7) were comparable to those from 2B5.

3.2.2 Methane Production in CSTRs

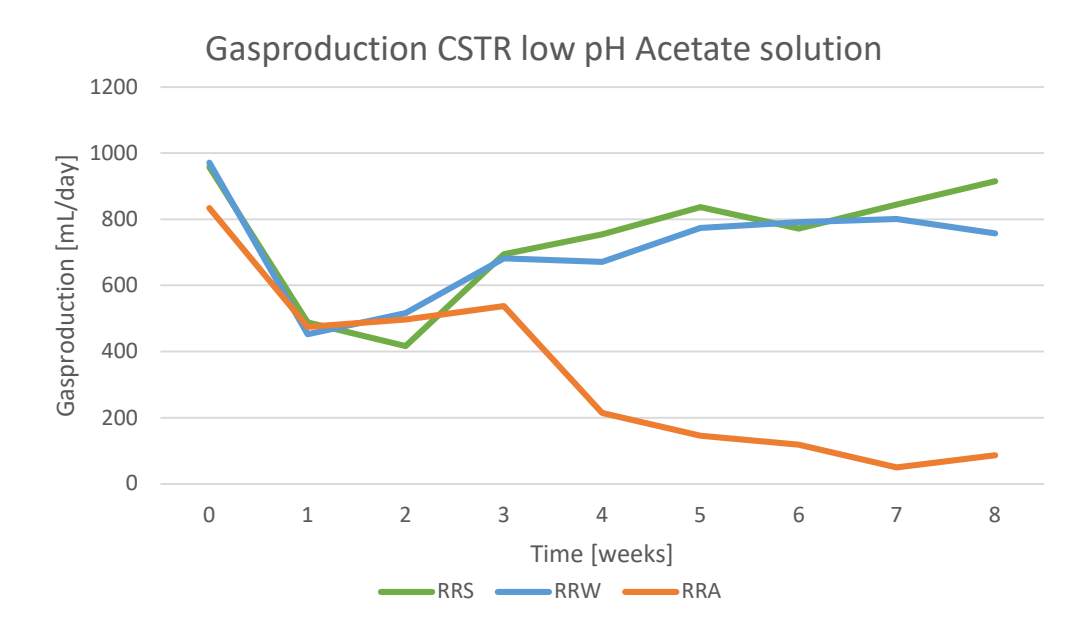


Figure 16 Gas production rates in a CSTR operated with low pH acetate solution over eight weeks. Shown are RRS (green), RRW (blue), and REA (yellow).

Gas production in RRA declined steadily over time, while RRS and RRW stabilized after the initial decrease. The Acetate enriched solution (TBR1-Ac)was from TBR 1.

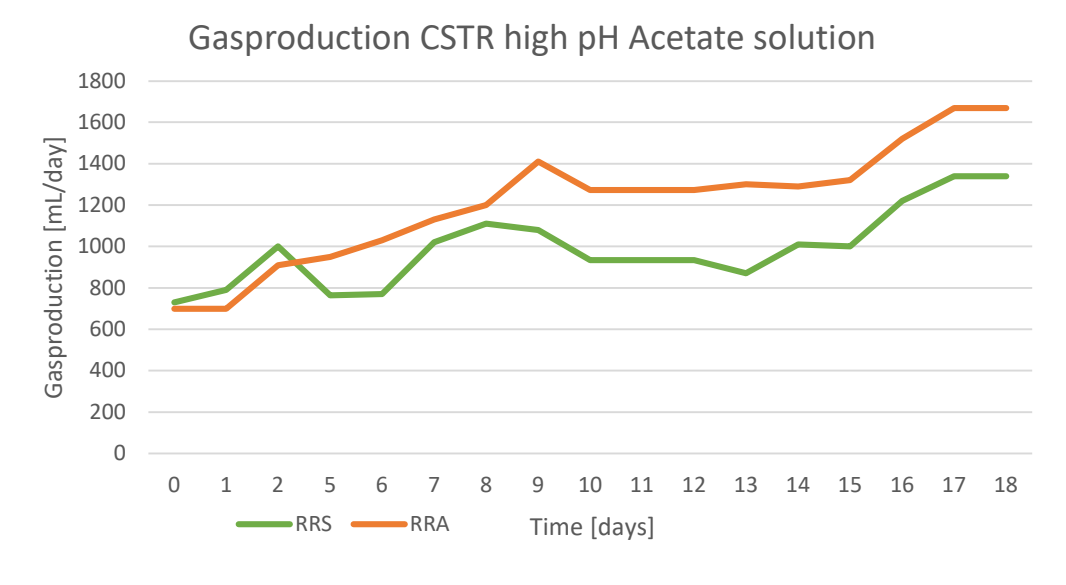


Figure 17 Gas production rates in a CSTR with high pH acetate solution over 18 days. Shown are RRS (blue) and RRA (orange).

At 21.05.25 the RRW was changed to the RRA. Gas production increased steadily increasing in both CSTRs throughout the experiment, with RRA achieving higher rates. In the high pH experiment, the TBR2-AC 2B4 solution was used from 21.5 to 30.5, and the TBR2-AC 2B5 solution from 31.5 to 8.6. Gas production in the RRA variant was 22.42% (t.test between RRS and RRA p=0.0058) higher compared to RRS during the observation period from 21.05 to 8.06.

3.2.3 Volumetric methane production

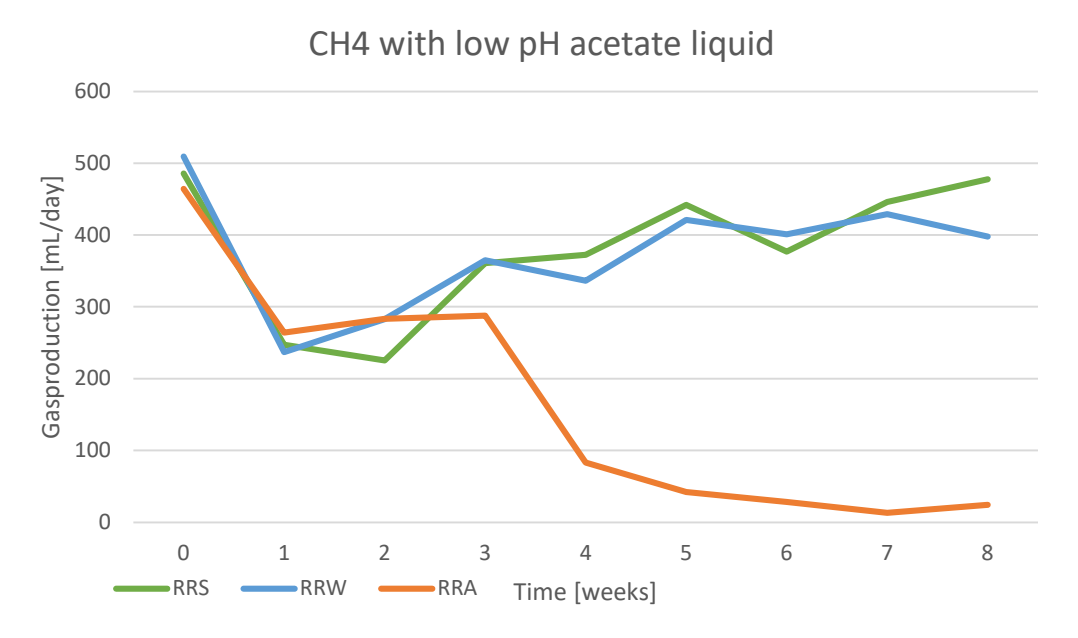


Figure 18 CH_4 production over time in reactors fed with low-pH acetate solution. The graph shows daily CH_4 production (mL/day) over 8 weeks for RRS (green), RRW (blue), and RRA (orange).

While CH₄ concentrations in RRS and RRW remained relatively stable throughout the experimental period, a continuous decline was observed in RRA. This is also reflected in the CH₄ values in the appendix 8, which show a drop to a minimum of 26.4% CH₄ content in week 5.

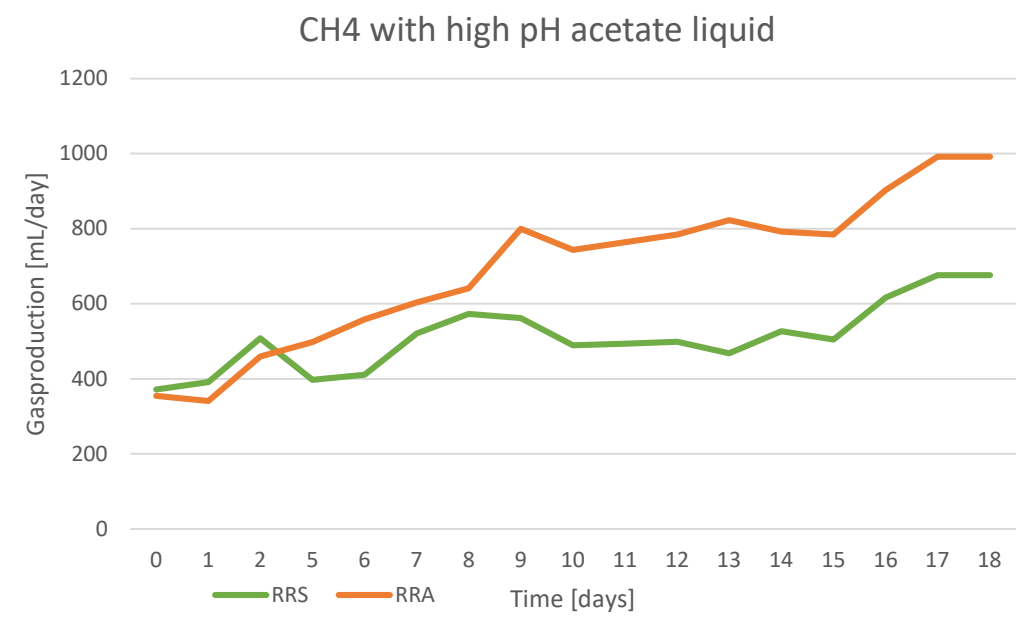


Figure 19 CH_4 production over time in reactors fed with high-pH acetate solution. The graph shows daily CH_4 production (mL/day) over 18 days for RRS (green) and RRA (orange).

CH₄ production increased in both reactors over the 18-day period with high-pH acetate solution. RRA reached approximately $1000 \,\mathrm{mL/day}$ by day 18, starting from around $350 \,\mathrm{mL/day}$. RRS increased from about $400 \,\mathrm{mL/day}$ to approximately $670 \,\mathrm{mL/day}$. RRA maintained higher values than RRS throughout the measurement period. The CH₄ level see appendix 8 remained stable throughout the experiment, while RRA showed a continuous increase, peaking above 60% towards the end of the observation period. The measured CH₄ values for dates without recorded data were linearly interpolated. In total a 36% higher production of CH₄ volume could be achieved compared to the RRS (t.test; p = 0.0022 between RRS and RRA; Annova F = 12.12 and p = 0.000055).

4. Discussion

4.1 Utilizing Acetate-Rich Substrates in CSTR

Recent studies (Bassani et al., 2015; Devarapalli et al., 2016; Szuhaj et al., 2016; Corbellini et al., 2021) have revealed that integrating products from TBRs into CSTRs is an effective strategy for increasing gas production and improved energy yields. During the first few days after 100 g of TBR1-Ac was inserted into the stable operating CSTRs, the RRA first indicated an increase in gas production. But after the short increase, the reactor's instability grew. This pattern is depicted in Figure 16, which shows a strong decline in gas production after an upward trend. CH4 levels showed similar dynamics, declining over the same time period (see Figure 18). The main reason of this decline was the addition of TBR1-Ac, which caused contamination with the known methanogen inhibitor 2-BES (Zinder, Anguish and Cardwell, 1984; Qiu et al., 2023). Additional contributing factors, cannot be excluded.

The experiment was repeated by using RRW as the Acetate reactor at the 21.05.25 instead of RRA after a contamination—likely brought on by 2-BES—in the RRA reactor. Following this, RRW acquired a new role and operated as the RRA. It was then fed 100 g of TBR 2's acetate-enriched liquid. Feeding the reactor TBR2-Ac produced higher gas production compared to the TBR1-Ac experiment. Gas production increased, as seen in figure 17 with RRA obtaining a yield that was 22.4% greater than that of the reference reactor RRS. Figure 19 shows an increase in volumetric CH₄ production, driven by the higher CH₄ content of the gas. This resulted in a 36% greater CH₄ volume compared to the RRS. The CH₄ content also has room for improvement; the maximum value of 63.4% could be increased to up to 90% compared to the literature (Bassani *et al.*, 2015).

The calculations for gas production in Table 3 predicted increases ranging from 27% to 113%, depending on the acetate input. The measured gas output remained below the values estimated by calculation, which based on a standard CH₄ content of 60%. At this assumed CH₄ level, the observed 36% increase would result in a higher calculated output, or conversely, the initial estimates would need to be adjusted downward. Possible biological reasons could be an inadequate reaction time for the full turnover of the substrate, the presence of inhibitory compounds, or unknown process bottlenecks.

With the initial idea of energy transferring into biogas for storing seems to be possible, but with efficiency and time limitations. In contrast to normal feeding, no increase in gas production was observed at the start of feeding. Fast gas production initially after feeding was not observed, but slightly higher production after the weekend. A slow degradation and accumulation of VFA could be a reason for that. High concentrations of acetate can inhibit hydrogen production, as seen in studies where the ratio of ethanol to acetic acid was critical for optimizing hydrogen yields (Divya, Gopinath and Merlin Christy, 2015; Krishnan *et*

al., 2017) The long-term effects of such inhibition remain unclear and warrant further investigation. Additional research is needed to determine the acetate concentration at which gas production reaches its maximum and their effect on CSTRs.

4.2 Performance Constraints and Enhancements in TBR

When comparing the two TBR reactors directly, as illustrated in Figure 8 with the two best-performing curves, it is visible that TBR2 generated a higher acetate concentration under almost the same operating conditions. TBR2's peak acetate concentration was nearly an order of magnitude higher than TBR1's after the same time amount. This difference demonstrates that TBR2's process environment was more advantageous to the formation of acetate than from TBR1. This pattern can also be observed in the two continuous operation curves shown in Figures 6 and 7. In TBR1 (Figure 6), the trend of the curve becomes negative after an initial increase during the first 16 days. In contrast, the trend in TBR2 (Figure 7) remains positive throughout the observed period. Compared to values reported in the literature and shown in Figure 9, the performance of TBR2 falls within the same range as other studies, even when accounting for the identified limitations. On its best day, TBR2 reached an acetate production rate of 3.53 g/L/day, as indicated in Table 2 and Figure 10.

There are probably multiple reasons for TBR1's lower performance. Contamination incidents, temperature variations, and issues with the temperature control and pH level are all potential sources of disruption. It is well known that even slight changes in pH or temperature can have a negative impact on microbial activity, which can then greatly hinder the expected acetate production (Xu *et al.*, 2015; Steger *et al.*, 2022; Hiebl *et al.*, 2025).

As compared to TBR2, TBR1 was first inoculated with a pre-adapted culture. This did not result in a better outcome, but could partly explain the highest curve 1B0 of TBR1. The inoculum in the column of the reactor could have died off after the first curve, or it was unable to form a strong microbial community because it was less resistant to environmental perturbations, especially temperature changes. In both reactors, a stable biofilm growth can enhance the TBR process even further(Devarapalli *et al.*, 2016; Rachbauer *et al.*, 2016). Higher conversion rates are promoted by carriers which provide an accessible surface area, which enables microbial attachment and the formation of stable biofilms. This will result in greater retention of biomass.

Another important aspect is to maintain pH within an ideal range. Based on previous studies, pH levels below 5.5 typically prevent chain elongation and reduce the yields of longer-chain products. Also, a neutral pH of 7 produces the greatest quantity of acetate (Xu et al., 2015; Steger et al., 2022; Hiebl et al., 2025). At neutral pH, the highest microbial diversity is usually reported. Figure 11 illustrates that, in the acidic pH conditions around 6, the number of acetate producers was relatively low and the diversity of acids was higher. TBR 2 demonstrated a higher quantity of acetate-producing organisms but a lower overall

diversity, according to the acid composition analysis shown in Figures 12 and 13. The amount of isovalerate was higher in TBR1 to TBR2. Both reactors experienced pH fluctuations within a range of about 0.5 pH units as a result of the constant addition of sodium hydroxide to stabilize the pH. Monitoring of process variables such as pH, redox potential, and gas composition is necessary to spot disturbances early and maintain the intended metabolic pathways (Amani, Nosrati and Sreekrishnan, 2010).

Stability of temperature turned out to be an especially critical factor. This is probably one of the primary causes of TBR 1 malfunctions and can be seen in changes in the gas outflow to the security control. Although thermophilic conditions have been shown to promote acidogenesis, some researchers have pointed out that they may also threaten the survival of methanogenic archaea while making reactor management more difficult (Steger *et al.*, 2022; He *et al.*, 2025).

As shown in Figure 14, the initial phase of CH₄ production after a new batch without 2-BES was implemented on 10.04.25 was another limitation identified in TBR 1. Particularly in situations with limited nutrients, methanogens are more effective competitors for available substrates than acetogens (Schnürer, 2018). Consequently, the intended process is disrupted as hydrogen and CO₂ are more frequently converted to CH₄ rather than acetate. Although methanogenesis could be inhibited by adding 2-BES, this strategy is not practical in the current system because of possible adverse effects on the CSTR process. Alternatively, since methanogens typically cannot survive at lower pH levels, operating at a pH below 5.8 may suppress methanogen activity. Figure 15 shows that CH₄ was produced in TBR 2 during the acetate production phase. This likely led to a reduction in available hydrogen and acetate for acidogenesis. To limit methanogenic activity and support acetate accumulation, the pH was increased for further research to 9.3.

4.3 Literature Comparison and Limitations of TBR Performance

The thesis's outcomes demonstrate that, in alkaline environments, TBRs can efficiently convert hydrogen and CO2 into acetic acid. The reactor reached a maximum production rate of 3.83 g/L per day and an acetic acid concentration of 12.4 g/L under operating conditions of 52 °C and pH 8.7–9.0.

These findings align with characteristics from literature, though different TBR systems show varying operational and performance limitations. For instance, Steger et al. (2022) carried out acetogenic H_2/CO_2 conversion in TBRs at $30 \pm 1^{\circ}C$ with the objective of keeping the pH at 7.0 ± 0.3 by adding sodium hydroxide every day (Steger *et al.*, 2022). Devarapalli et al. (2016) demonstrated syngas fermentation in trickle-bed reactors at $37^{\circ}C$. In their setup, the pH was set to 5.8 but gradually decreased to around 4.6 due to the accumulation of acetic acid and the lack of pH regulation. Under these conditions and with cocurrent gas flow, acetic acid concentrations reached up to 12.3 g/L (Devarapalli *et al.*, 2016). Hiebl et al. (2025) conducted a study on TBRs for chain elongation at a temperature of $30^{\circ}C$, with pH values set between 6.0 and 6.5. Production of butyrate and caproate peaked at pH 6.0, with produces sharply decreasing at pH 5.3 and lower (Hiebl *et al.*, 2025). By using chain-elongating bacteria for targeted bioaugmentation, microbial communities can be guided toward the production of longer-chain fatty acids (Hiebl et al., 2025; Dyksma et al., 2020).

From a technical point, each study identifies the operational constraints that include the risks of biofilm detachment and clogging, channelling within the packed bed, uneven liquid distribution, and limitations in gas-liquid mass transfer. At larger scales, the solubility of H₂ and CO, along with the inherently complex hydrodynamics of TBRs, could create engineering challenges (Mederos, Ancheyta and Chen, 2009). Another test is to maintain a high cell density and avoid nutrient depletion, which makes frequent medium exchange important to prevent substrate limitation and cell washout during continuous operation (Steger et al., 2022). This depends strongly on the type of carrier material used. Differences in inoculum preparation and medium exchange techniques make it more difficult to directly compare TBR experiments. Process stability and productivity can be greatly impacted by variations in the microbial community at the beginning of each experiment as well as variations in the frequency and timing of medium replacement (Devarapalli et al., 2016; Steger et al., 2022; Hiebl et al., 2025). Parameters such as temperature, pH, inoculum preparation, microbial community choice, carrier material selection, and medium exchange influence reactor performance. Optimized reactor design is critical to unlocking their full potential This study demonstrated that high alkalinity and an operating temperature of 52 °C support acetate production in TBRs; however, further research is needed to define optimal operational ranges and ensure process stability for varying application objectives.

5. Conclusion and Future prospects

This study evaluated the potential of a PtG approach—converting electrical energy into hydrogen, then into acetate, and finally into CH₄—to enhance the efficiency and flexibility of energy systems in the context of renewable integration and climate change mitigation. To investigate this, the study was divided into two parts: (1) the production of VFAs, primarily acetate, from hydrogen and CO₂ in a TBR, and (2) the subsequent use of acetate-enriched substrate in a CSTR for CH₄ production.

In the first part, the conversion of hydrogen to acetate was demonstrated under alkaline conditions. Best production occurred at a temperature of 52 °C and a pH range of 8.7–9.0. Under these conditions, TBR 2 achieved an acetic acid concentration of 12.4 g/L and a maximum production rate of 3.83 g/L per day. Additionally, elevated VFA concentrations were detected, with lower pH levels promoting the formation of other acids such as propionate, valerate and butyrate

The second part focused on the use of acetate-enriched liquid as a substrate in the CSTR. Compared to the reference reactors, the acetate-fed system demonstrated improved CH₄ yields. Visible in Figure 19, the CH₄ production increased significant by 36% relative to the RRS control, indicating a potential for upgrading fluctuating electricity into storable acetate energy via microbial processes.

The results indicate that the approach tested in this study is achievable, overall visible with good CH₄ production rates. Nonetheless, further potential exists, as suggested by comparisons with previously published data. The CH₄ quality values could be further enhanced by acetate and the overall production of gas increased. Acetate-rich liquids, as produced more efficiently in the alkaline TBR system, prove the ability to serve as suitable substrates for CH₄ generation. These also have potential for growth. The results also show that such acetate solutions can be obtained without the need for antifoam agents or acidifiers such as HCl or H₃PO₄, making the process more cost-efficient. This method, after further validation, may be applicable in industrial settings, such as the biogas facility in Linköping. However, several aspects require clarification. Both the maximum allowable acetate concentration in the CSTR and the system's reaction to increased acetate loadings are still not known. To evaluate long-term impacts on microbial stability and process efficiency, the CSTR experiment must be extended beyond a single HRT.

To better integrate microbial PtG systems into the present biogas infrastructure, future studies should concentrate on long-term stability, scale-up potential, and process parameter tuning. Overall, this thesis supports the potential of microbial PtG as a flexible and sustainable component in the future energy landscape..

References

- Amani, T., Nosrati, M. and Sreekrishnan, T.R. (2010) 'Anaerobic digestion from the viewpoint of microbiological, chemical, and operational aspects a review', *Environmental Reviews*, 18(NA), pp. 255–278. Available at: https://doi.org/10.1139/A10-011.
- Bajpai, P. (2017) 'Basics of Anaerobic Digestion Process', in Bajpai, P., *Anaerobic Technology in Pulp and Paper Industry*. Singapore: Springer Singapore (SpringerBriefs in Applied Sciences and Technology), pp. 7–12. Available at: https://doi.org/10.1007/978-981-10-4130-3 2.
- Bakkaloglu, S. and Hawkes, A. (2024) 'A comparative study of biogas and biomethane with natural gas and hydrogen alternatives', *Energy & Environmental Science*, 17(4), pp. 1482–1496. Available at: https://doi.org/10.1039/D3EE02516K.
- Bassani, I. et al. (2015) 'Biogas Upgrading via Hydrogenotrophic Methanogenesis in Two-Stage Continuous Stirred Tank Reactors at Mesophilic and Thermophilic Conditions', *Environmental Science & Technology*, 49(20), pp. 12585–12593. Available at: https://doi.org/10.1021/acs.est.5b03451.
- Corbellini, V. *et al.* (2021) 'Performance Analysis and Microbial Community Evolution of In Situ Biological Biogas Upgrading with Increasing H2/CO2 Ratio', *Archaea*. Edited by R. Amils, 2021, pp. 1–15. Available at: https://doi.org/10.1155/2021/8894455.
- Cuff, G. *et al.* (2020) 'Production and upgrading of biogas through controlled hydrogen injection for renewable energy storage', *Bioresource Technology Reports*, 9, p. 100373. Available at: https://doi.org/10.1016/j.biteb.2019.100373.
- Cui, W., Luo, H. and Liu, G. (2023) 'Efficient hydrogen production in single-chamber microbial electrolysis cell with a fermentable substrate under hyperalkaline conditions', *Waste Management*, 171, pp. 173–183. Available at: https://doi.org/10.1016/j.wasman.2023.08.017.
- Dao, H. and Friot, D. (2025) 'Planetary Boundaries: designing (fair?) limits to assess performance at the country level', *Frontiers in Sustainable Resource Management*, 4, p. 1537031. Available at: https://doi.org/10.3389/fsrma.2025.1537031.
- Davies, E., Ehrmann, A. and Schwenzfeier-Hellkamp, E. (2024) 'Safety of Hydrogen Storage Technologies', *Processes*, 12(10), p. 2182. Available at: https://doi.org/10.3390/pr12102182.
- Devarapalli, M. *et al.* (2016) 'Ethanol production during semi-continuous syngas fermentation in a trickle bed reactor using Clostridium ragsdalei', *Bioresource Technology*, 209, pp. 56–65. Available at: https://doi.org/10.1016/j.biortech.2016.02.086.
- Divya, D., Gopinath, L.R. and Merlin Christy, P. (2015) 'A review on current aspects and diverse prospects for enhancing biogas production in sustainable means', *Renewable and Sustainable Energy Reviews*, 42, pp. 690–699. Available at: https://doi.org/10.1016/j.rser.2014.10.055.

Dupont, C. *et al.* (2024) 'Three decades of EU climate policy: Racing toward climate neutrality?', *WIREs Climate Change*, 15(1), p. e863. Available at: https://doi.org/10.1002/wcc.863.

Dyksma, S., Jansen, L. and Gallert, C. (2020) 'Syntrophic acetate oxidation replaces acetolactic methanogenesis during thermophilic digestion of biowaste', *Microbiome*, 8(1), p. 105. Available at: https://doi.org/10.1186/s40168-020-00862-5.

Farghali, M. *et al.* (2022) 'Integration of biogas systems into a carbon zero and hydrogen economy: a review', *Environmental Chemistry Letters*, 20(5), pp. 2853–2927. Available at: https://doi.org/10.1007/s10311-022-01468-z.

Fu, B. *et al.* (2019) 'Competition Between Chemolithotrophic Acetogenesis and Hydrogenotrophic Methanogenesis for Exogenous H2/CO2 in Anaerobically Digested Sludge: Impact of Temperature', *Frontiers in Microbiology*, 10, p. 2418. Available at: https://doi.org/10.3389/fmicb.2019.02418.

Fujimura, D. and Matsumoto, K. (2021) 'C190-E263 Technical Report: Simple Method Transfer using i-Series (LC-2050/LC-2060)'.

Fukuzumi, S. (ed.) (2020) 'Hydrogen Storage', in *Electron Transfer*. 1st edn. Wiley, pp. 93–108. Available at: https://doi.org/10.1002/9783527651771.ch8.

Geotech (2015) 'BIOGAS 5000 User Manual.' A QED Environmental Systems Company. Available at: https://www.envirotecnics.com/en/product/biogas-5000-analyzer/#documents.

Hach (2025) 'AT1000 Series Automatic Titrator – User Manual'. Available at: https://cdn.hach.com/7FYZVWYB/at/37vtwvtz39vq4cks5kk59xj3/DOC0225293 074 11ed.pdf.

He, H. *et al.* (2025) 'A review of temperature and key parameters influencing the hydrolysis-methanogenesis balance in anaerobic digestion', *Fuel*, 394, p. 134927. Available at: https://doi.org/10.1016/j.fuel.2025.134927.

Hiebl, C. et al. (2025) 'Enhancing Gas Fermentation Efficiency via Bioaugmentation with Megasphaera succiensis and Clostridium carboxidivorans', *Bioengineering*, 12(5), p. 470. Available at: https://doi.org/10.3390/bioengineering12050470.

Kern, T. *et al.* (2016) 'Assessment of hydrogen metabolism in commercial anaerobic digesters', *Applied Microbiology and Biotechnology*, 100(10), pp. 4699–4710. Available at: https://doi.org/10.1007/s00253-016-7436-5.

Kim, S. *et al.* (2021) 'Production of high-calorific biogas from food waste by integrating two approaches: Autogenerative high-pressure and hydrogen injection', *Water Research*, 194, p. 116920. Available at: https://doi.org/10.1016/j.watres.2021.116920.

Klueber, H.D. and Conrad, R. (1998) 'Effects of nitrate, nitrite, NO and N2O on methanogenesis and other redox processes in anoxic rice field soil', *FEMS Microbiology Ecology*, 25(3), pp. 301–318. Available at: https://doi.org/10.1111/j.1574-6941.1998.tb00482.x.

Krishnan, S. et al. (2017) 'An investigation of two-stage thermophilic and mesophilic fermentation process for the production of hydrogen and methane from palm oil mill effluent', *Environmental Progress & Sustainable Energy*, 36(3), pp. 895–902. Available at: https://doi.org/10.1002/ep.12537.

Lili, M. et al. (2011) 'NOVEL APPROACH ON THE BASIS OF FOS/TAC METHOD'.

Löw, R. (2024) 'In-situ methanation of hydrogen', *Environmental Change* [Preprint].

Luo, G. *et al.* (2012) 'Simultaneous hydrogen utilization and in situ biogas upgrading in an anaerobic reactor', *Biotechnology and Bioengineering*, 109(4), pp. 1088–1094. Available at: https://doi.org/10.1002/bit.24360.

Mederos, F.S., Ancheyta, J. and Chen, J. (2009) 'Review on criteria to ensure ideal behaviors in trickle-bed reactors', *Applied Catalysis A: General*, 355(1–2), pp. 1–19. Available at: https://doi.org/10.1016/j.apcata.2008.11.018.

Ni, M. (2006) 'An Overview of Hydrogen Storage Technologies', *Energy Exploration & Exploitation*, 24(3), pp. 197–209. Available at: https://doi.org/10.1260/014459806779367455.

PerkinElmer (2017) 'Clarus 590 Gas Chromatograph Specifications'. Available at: https://perkinelmer.com.ar/wp-content/uploads/sites/3/2018/08/Clarus-590-GC-Specification-Sheet.pdf.

Phenomenex (2025) Rezex ROA-Organic Acid H+ (8%) Ion Exclusion HPLC Columns, Phenomenex. Available at: https://www.phenomenex.com/prod-ucts/rezex-hplc-column/rezex-roa-organic-acid-h (Accessed: 4 May 2025).

Qiu, S. *et al.* (2023) 'Impacts of 2-bromoethanesulfonic sodium on methanogenesis: Methanogen metabolism and community structure', *Water Research*, 230, p. 119527. Available at: https://doi.org/10.1016/j.watres.2022.119527.

Rachbauer, L. *et al.* (2016) 'Biological biogas upgrading capacity of a hydrogenotrophic community in a trickle-bed reactor', *Applied Energy*, 180, pp. 483–490. Available at: https://doi.org/10.1016/j.apenergy.2016.07.109.

Rampai, M.M. *et al.* (2024) 'Hydrogen production, storage, and transportation: recent advances', *RSC Advances*, 14(10), pp. 6699–6718. Available at: https://doi.org/10.1039/D3RA08305E.

Salehi, J. et al. (2022) 'Effect of power-to-gas technology in energy hub optimal operation and gas network congestion reduction', *Energy*, 240, p. 122835. Available at: https://doi.org/10.1016/j.energy.2021.122835.

Saltnes, T., Eikebrokk, B. and Ødegaard, H. (2002) 'Contact filtration of humic waters: performance of an expanded clay aggregate filter (Filtralite) compared to a dual anthracite/sand filter', *Water Supply*, 2(5–6), pp. 17–23. Available at: https://doi.org/10.2166/ws.2002.0145.

Salvetti, F. et al. (2023) 'The e-REAL's Time Travelling Immersive Experience Towards a Net-Zero Greenhouse Gas Emissions Economy', *International Journal of Advanced Corporate Learning (iJAC)*, 16(3), pp. 60–72. Available at: https://doi.org/10.3991/ijac.v16i3.35743.

- Schnürer, A. (2018) Microbiology of the biogas process.
- Siegel, R.S. and Ollis, D.F. (1984) 'Kinetics of growth of the hydrogen-oxidizing bacterium *Alcaligenes eutrophus* (ATCC 17707) in chemostat culture', *Biotechnology and Bioengineering*, 26(7), pp. 764–770. Available at: https://doi.org/10.1002/bit.260260721.
- Sikora, A. *et al.* (2017) 'Anaerobic Digestion: I. A Common Process Ensuring Energy Flow and the Circulation of Matter in Ecosystems. II. A Tool for the Production of Gaseous Biofuels', in A.F. Jozala (ed.) *Fermentation Processes*. InTech. Available at: https://doi.org/10.5772/64645.
- Steger, F. *et al.* (2022) 'Trickle-Bed Bioreactors for Acetogenic H2/CO2 Conversion', *Frontiers in Energy Research*, 10, p. 842284. Available at: https://doi.org/10.3389/fenrg.2022.842284.
- Szuhaj, M. *et al.* (2016) 'Conversion of H2 and CO2 to CH4 and acetate in fedbatch biogas reactors by mixed biogas community: a novel route for the power-togas concept', *Biotechnology for Biofuels*, 9(1), p. 102. Available at: https://doi.org/10.1186/s13068-016-0515-0.
- Tg, I., Haq, I. and Kalamdhad, A.S. (2022) 'Factors affecting anaerobic digestion for biogas production: a review', in *Advanced Organic Waste Management*. Elsevier, pp. 223–233. Available at: https://doi.org/10.1016/B978-0-323-85792-5.00020-4.
- Tichler, R., Bauer, S. and Böhm, H. (2022) 'Power-to-Gas', in *Storing Energy*. Elsevier, pp. 595–612. Available at: https://doi.org/10.1016/B978-0-12-824510-1.00010-6.
- 'Uppsala vattens biogasanläggning' (2021).
- Vos, R. *et al.* (2025) 'Global shocks to fertilizer markets: Impacts on prices, demand and farm profitability', *Food Policy*, 133, p. 102790. Available at: https://doi.org/10.1016/j.foodpol.2024.102790.
- Xie, Z. *et al.* (2024) 'A Review of Hydrogen Storage and Transportation: Progresses and Challenges', *Energies*, 17(16), p. 4070. Available at: https://doi.org/10.3390/en17164070.
- Xu, S. *et al.* (2015) 'Bioconversion of H2/CO2 by acetogen enriched cultures for acetate and ethanol production: the impact of pH', *World Journal of Microbiology and Biotechnology*, 31(6), pp. 941–950. Available at: https://doi.org/10.1007/s11274-015-1848-8.
- Yu, J. and Munasinghe, P. (2018) 'Gas Fermentation Enhancement for Chemolithotrophic Growth of Cupriavidus necator on Carbon Dioxide', *Fermentation*, 4(3), p. 63. Available at: https://doi.org/10.3390/fermentation4030063.
- Zhang, L. (2023) 'Hydrogen Storage Methods, Systems and Materials', *High-lights in Science, Engineering and Technology*, 58, pp. 371–378. Available at: https://doi.org/10.54097/hset.v58i.10125.
- Zhu, X. et al. (2020) 'The role of endogenous and exogenous hydrogen in the microbiology of biogas production systems', World Journal of Microbiology and

Biotechnology, 36(6), p. 79. Available at: https://doi.org/10.1007/s11274-020-02856-9.

Zinder, S.H., Anguish, T. and Cardwell, S.C. (1984) 'Selective Inhibition by 2-Bromoethanesulfonate of Methanogenesis from Acetate in a Thermophilic Anaerobic Digestor', *Applied and Environmental Microbiology*, 47(6), pp. 1343–1345. Available at: https://doi.org/10.1128/aem.47.6.1343-1345.1984.

Appendix

Appendix table 1 CSTR data for the complet time period

		Measur	ed [mL]		Gascount with calibration [mL]			
Date	RRS	RRA		RW	RRS	RRA	RRW	
24.02.2025	-	-		760.0	13470.3	2279.8	75.7	
25.02.2025	-	-	_		739.1	863.6	37.9	
26.02.2025	-	-		1170.0	739.1	1796.2	113.6	
27.02.2025	-	-	-		457.5	310.9	75.7	
28.02.2025	-	-	-		633.5	241.7	75.7	
03.03.2025	-	-		3485.0	3273.1	2418.0	189.3	
04.03.2025	-	-	-		879.9	725.4	75.7	
05.03.2025	-	-	-		915.1	1036.3	189.3	
06.03.2025		-	-		1055.8	1105.3	37.9	
07.03.2025	-	-	-		1126.2	932.6	1755.0	
10.03.2025	-	-		3510.0	3554.6	3143.4	1755.0	
11.03.2025	-	-	-		1126.2	705.9	871.7	
12.03.2025	-	-	-		1231.8	621.8	871.7	
13.03.2025	-	-		2615.0	1055.8	276.4	871.7	
14.03.2025	-	-	-		1126.2	1140.0	75.7	
17.03.2025	-	-	-		3097.1	2728.9	2765.1	
18.03.2025	-	-	-		879.9	863.6	909.1	
19.03.2025		690.0	750.0	835.0	703.9	759.9	833.2	
20.03.2025	-	-	-		973.7	994.7	895.3	
21.03.2025	-	-	-		-	-	-	
24.03.2025	-	-	-		3308.3	3127.4	3560.5	
25.03.2025	-	-	-		1724.5	957.4	1515.1	
26.03.2025	-	-	-		797.7	574.4	707.1	
27.03.2025	-	-	-		844.7	957.4	795.5	
28.03.2025	-	-	-		950.3	989.3	909.1	
31.03.2025	-	-	-		821.2	797.8	757.6	
01.04.2025	-	-	-		-	-	-	
02.04.2025	-	-	-		281.6	765.9	795.5	
03.04.2025	-	-	-		668.2	670.2	719.6	
04.04.2025	-	-	-		739.1	765.9	795.5	
07.04.2025	-	-	-		740.1	765.9	808.1	
08.04.2025		450.0	490.0	470.0	492.7	510.6	492.5	
09.04.2025		574.0	640.0	635.0	633.5	638.3	644.0	
09.04.2025	-	-	-		739.1	734.0	719.6	
10.04.2025		505.0 -	-		563.1	638.3	492.5	
11.04.2025	-		700.0 -		703.9	734.0	681.8	
14.04.2025	-	-	-		2288.2	1436.0	2272.7	
15.04.2025	-	-	-		563.1	222.8	606.6	
16.04.2025	-	-	-		774.3	383.0	681.8	

17.04.2025		-	-	739.1	223.4	719.6
18.04.2025		-	-	598.3	255.3	
21.04.2025		-	-	2428.9	319.2	2614.0
22.04.2025		-	-	739.6	319.2	681.7
23.04.2025		-	-	739.1	567.3	681.8
24.04.2025		230.0		668.7		644.0
25.04.2025		190.0	800.0	809.5	191.4	833.3
28.04.2025	2330.0	230.0	2400.0	2604.4	223.4	2462.1
29.04.2025	740.0	40.0	730.0	1036.5		795.5
30.04.2025	690.0	420.0	721.0	663.1		688.7
01.05.2025		420.0		915.1		947.2
02.05.2025	-	1170.0	-	693.7	-	719.6
05.05.2025	2440.0	810.0	2160.0	2358.0	829.7	2424.2
06.05.2025	700.0	400.1	830.0	774.3	-	757.6
07.05.2025	600.0	330.0	690.0	668.7	-	719.6
08.05.2025	700.0	430.0	840.0	739.1	-	757.6
09.05.2025	830.0	370.0	860.0	844.7	351.0	871.2
12.05.2025	1880.0	1060.0	2450.0	2745.2	-	2537.9
13.05.2025	860.0	380.0	600.0	915.1	-	719.7
14.05.2025	800.0	250+70	740.0	844.7	223.4	681.8
15.05.2025	840.0	340.0	550.0	879.9	-	568.2
16.05.2025	1030.0	400.0	470.0	1091.0	383.0	984.8
19.05.2025	2340.0	860.0	2210.0	2674.8	-	2272.7
20.05.2025	830.0	390.0	830.0	915.1	-	795.5
	RRS	RRW	RRA	RRS	RRW	RRA
21.05.2025	730.0	120.0	700.0	774.3	95.8	681.8
22.05.2025	790.0	290.0	700.0	809.5	-	681.8
23.05.2025	1000.5	390.0	910.0	979.3	-	928.2
26.05.2025	763.3	143.3	950.0	2604.4	-	-
27.05.2025	770.0	380.0	1030.0	844.7	351.0	1098.5
28.05.2025	1020.0	650.0	1130.0	1055.8	670.2	1098.5
29.05.2025	1110.0	780.0	1200.0	1091.0	765.9	1174.3
30.05.2025	1080.0	940.0	1410.0	1196.6	925.5	1363.6
31.05.2025	933.3	963.3	1273.3	1184.9	999.9	1300.5
01.06.2025	933.3	963.3	1273.3	1184.9	999.9	1300.5
02.06.2025	933.3	963.3	1273.3	1184.9	999.9	1300.5
03.06.2025	870.0	1060.0	1300.0	915.1	1053.1	1136.3
04.06.2025	1010.0	1090.0	1290.0	1091.0	1117.0	1287.8
05.06.2025	1000.0	1130.0	1320.0	1091.0	1117.0	1249.9
06.06.2025	1220.0	1270.0	1520.0	1337.4	1244.6	1553.0
07.06.2025	1340.0	1410.0	1670.0	1555.7	1403.7	1609.9
08.06.2025	1340.0	1410.0	1670.0	1555.7	1403.7	1609.9

Appendix table 2 TS/VS for all materials

Datum	Prov	rep	Tara	Tara+prov	prov	tara+ts	ts	tara+ash	ash	TS	TS avg.	VS	VS avg.	STDEV	STDEV-%
		a	3.199	77.099	73.900	5.844	2.645	4.044	0.845	3.58%		2.44%			
		b	3.186	79.401	76.215	5.938	2.752	4.069	0.883	3.61%		2.45%			
26.02.2025	Uppsala Biogas plant Substrat	c	3.206	80.585	77.379	5.999	2.793	4.100	0.894	3.61%	3.60%	2.45%	2.45%	0.000101414	0.41%
		a	3.188	105.167	101.979	7.292	4.104	4.402	1.214	4.02%		2.83%			
		b	3.173	104.682	101.509	7.252	4.079	4.390	1.217	4.02%		2.82%			
26.02.2025	Uppsala Biogas plant digestate main reactor	c	3.188	102.636	99.448	7.172	3.984	4.360	1.172	4.01%	4.02%	2.83%	2.83%	7.25078E-05	0.26%
		a	3.231	89.533	86.302	4.939	1.708	3.795	0.564	1.98%		1.33%			
21.05.2025	Filtered Substrate	b	3.202	92.124	88.922	4.968	1.766	3.793	0.591	1.99%	1.98%	1.32%	1.32%	2.9662E-05	0.22%
		a	3.220	100.839	97.619	7.753	4.533	4.594	1.374	4.64%		3.24%			
21.05.2025	Digestate of main reactor new	b	3.226	111.019	107.793	8.249	5.023	4.745	1.519	4.66%	4.65%	3.25%	3.24%	0.000103411	0.32%
		a	3.208	89.601	86.393	6.697	3.489	4.246	1.038	4.04%		2.84%			
21.05.2025	Digestate of main reactor old	b	3.217	84.933	81.716	6.509	3.292	4.201	0.984	4.03%	4.03%	2.82%	2.83%	8.92308E-05	0.32%

Appendix table 3 Hydraulic retention time of the CSTR

Hydraulic retention time								
Volume [mL]		5400						
Feeding [g]	100+304.4	404.40						
Weekend factor		1.4						
Time [days]		18.69						

Appendix table 4 TBR1 VFA g/L

	Acetate	Prop	pionate	IsoButyrate	Butyrate	IsoValerate
	atch [g/L]	[g/L	-	[g/L]	[g/L]	[g/L]
		0.12	0.01	0.35	0.072	0.033
21.03.2025 1H		.665	0.037	0.038	0.113	0.079
		.759	0.069	0.052	0.137	0.106
25.03.2025 1H		.902	0.108	0.05	0.105	0.148
		.064	0.099	0.061	0.116	0.126
		.078	0.1155	0.054	0.108	0.233
		.175	0.121	0.064	0.121	0.133
31.03.2025 1H	B0 1	.238	0.118	0.066	0.125	0.145
01.04.2025 1H	B0	1.11	0.1	0.115	0.111	0.363
02.04.2025 1H	B0 1	.485	0.142	0.073	0.136	0.336
03.04.2025 1H	B1 0	.053	0.061	0.049	0.074	0.103
03.04.2025 1H	B1 0	.347	0.093	0.204	0.082	0.111
04.04.2025 1H	B1 0	.428	0.09	0.057	0.115	0.116
07.04.2025 1H	B1 0	.675	0.086	0.141	0.294	0.868
08.04.2025 1H	B1 0	.861	0.078	0.003	0.078	0
09.04.2025 1H	B1 0	.638	0.039	0.078	0.038	0.047
10.04.2025 1H	B1 0	.973	0.088	0.033	0.083	0.045
11.04.2025 1H	B1 0	.743	0.081	0.008	0.084	0.043
14.04.2025 1H	B1 0	.586	0.051	0.079	0.062	0.076
16.04.2025 1H	B1 1	.047	0.1	0.12	0.1	0.095
17.04.2025 1H	B1 0	.714	0.064	0.109	0.067	0.085
22.04.2025 1H	B2 0	.213	0.047	0.129	0.046	0.046
23.04.2025 1H	B2 0	.353	0.083	0.134	0.077	0.06
24.04.2025 1H	B2 0	.342	0.107	0.035	0.103	0.094
25.04.2025 1H	B2 0	.433	0.182	0.459	0.212	0.135
28.04.2025 1H	B2 0	.427	0.174	0.298	0.202	0.137
06.05.2025 1H		.556	0.262	0.073	0.273	0.153
08.05.2025 1H		.556	0.274	0.563	0.334	0.155
12.05.2025 1H		.342	0.176	0.036	0.184	0.096
13.05.2025 1H	-	.292	0.159	0.828	0.222	0.061
		.025	0.133	0.020	0.009	0
		0.03	0.001	0	0	0
15.05.2025 1H	-	.113	0.075	0.025	0.098	0.016

19.05.2025 1B6	0.142	0.069	0.045	0.108	0.018
20.05.2025 1B6	0.174	0.112	0	0.146	0.03
21.05.2025 1B6	0.238	0.155	0.014	0.175	0.063
27.05.2025 1B6	0.187	0.13	0.017	0.088	0.083
28.05.2025 1B6	0.208	0.135	0.037	0.069	0.071
29.05.2025 1B6	0.167	0.103	0.041	0.051	0.058
30.05.2025 1B6	0.222	0.144	0.025	0.066	0.076
02.06.2025 1B6	0.229	0.127	0.043	0.055	0.07

Appendix table 5 TBR 2 VFA g/L

	D . 1	Acetate	Propionate	-	Butyrate	IsoValerate
Date	Batch	[g/L]	[g/L]	[g/L]	[g/L]	[g/L]
12.05.2025	2B4	0.005	0.000	0.021	0.003	0.001
13.05.2025	2B4	0.010	0.001	0.041	0.006	0.002
14.05.2025	2B4	0.016	0.001	0.041	0.006	0.004
15.05.2025	2B4	0.025	0.003	0.043	0.006	0.006
19.05.2025	2B4	0.053	0.004	0.049	0.006	0.009
20.05.2025	2B4	0.092	0.005	0.049	0.006	0.011
21.05.2025	2B4	0.190	0.007	0.049	0.006	0.015
21.05.2025	2B5	0.255	0.008	0.056	0.006	0.017
22.05.2025	2B5	0.331	0.012	0.062	0.009	0.021
26.05.2025	2B5	0.495	0.013	0.062	0.009	0.024
27.05.2025	2B5	0.777	0.013	0.069	0.010	0.028
28.05.2025	2B5	1.166	0.014	0.072	0.011	0.033
28.05.2025	2B5	1.577	0.015	0.074	0.013	0.039
28.05.2025	2B7	1.672	0.015	0.074	0.013	0.040
29.05.2025	2B7	1.766	0.015	0.074	0.013	0.049
30.05.2025	2B7	1.933	0.015	0.079	0.014	0.051
02.06.2025	2B7	2.210	0.016	0.086	0.016	0.055

Date	Batch	Acetate (C2)	Propionate (C3)	IsoButy- rate (C4)	Butyrate (C4)	IsoVale- rate (C5)	VFA-C total
17.03.2025	1B0	0.004	0.000	0.016	0.003	0.002	0.025
21.03.2025	1B0	0.022	0.001	0.002	0.005	0.004	0.034
24.03.2025	1B0	0.025	0.003	0.002	0.006	0.005	0.042
25.03.2025	1B0	0.030	0.004	0.002	0.005	0.007	0.049
26.03.2025	1B0	0.035	0.004	0.003	0.005	0.006	0.054
27.03.2025	1B0	0.036	0.005	0.002	0.005	0.011	0.059
28.03.2025	1B0	0.039	0.005	0.003	0.005	0.007	0.059
31.03.2025	1B0	0.041	0.005	0.003	0.006	0.007	0.062
01.04.2025	1B0	0.037	0.004	0.005	0.005	0.018	0.069
02.04.2025	1B0	0.049	0.006	0.003	0.006	0.016	0.081
03.04.2025	1B1	0.002	0.002	0.002	0.003	0.005	0.015
03.04.2025	1B1	0.012	0.004	0.009	0.004	0.005	0.034
04.04.2025	1B1	0.014	0.003	0.003	0.005	0.006	0.031
07.04.2025	1B1	0.022	0.003	0.006	0.013	0.042	0.088
08.04.2025	1B1	0.029	0.003	0.000	0.004	0.000	0.036
09.04.2025	1B1	0.021	0.002	0.004	0.002	0.002	0.030
10.04.2025	1B1	0.032	0.004	0.001	0.004	0.002	0.043
11.04.2025	1B1	0.025	0.003	0.000	0.004	0.002	0.034
14.04.2025	1B1	0.020	0.002	0.004	0.003	0.004	0.032
16.04.2025	1B1	0.035	0.004	0.005	0.005	0.005	0.054
17.04.2025	1B1	0.024	0.003	0.005	0.003	0.004	0.039
22.04.2025	1B2	0.007	0.002	0.006	0.002	0.002	0.019
23.04.2025	1B2	0.012	0.003	0.006	0.003	0.003	0.028
24.04.2025	1B2	0.011	0.004	0.002	0.005	0.005	0.027
25.04.2025	1B2	0.014	0.007	0.021	0.010	0.007	0.059
28.04.2025	1B2	0.014	0.007	0.014	0.009	0.007	0.051
06.05.2025	1B3	0.019	0.011	0.003	0.012	0.007	0.052
08.05.2025	1B3	0.019	0.011	0.026	0.015	0.008	0.078
12.05.2025	1B3	0.011	0.007	0.002	0.008	0.005	0.033
13.05.2025	1B3	0.010	0.006	0.038	0.010	0.003	0.067
13.05.2025	1B6	0.001	0.000	0.000	0.000	0.000	0.001
14.05.2025	1B6	0.001	0.000	0.000	0.000	0.000	0.001
15.05.2025	1B6	0.004	0.003	0.001	0.004	0.001	0.013
19.05.2025	1B6	0.005	0.003	0.002	0.005	0.001	0.015
20.05.2025	1B6	0.006	0.005	0.000	0.007	0.001	0.018
21.05.2025	1B6	0.008	0.006	0.001	0.008	0.003	0.026
27.05.2025	1B6	0.006	0.005	0.001	0.004	0.004	0.020
28.05.2025	1B6	0.007	0.005	0.002	0.003	0.003	0.021
29.05.2025	1B6	0.006	0.004	0.002	0.002	0.003	0.017
30.05.2025	1B6	0.007	0.006	0.001	0.003	0.004	0.021
02.06.2025	1B6	0.008	0.005	0.002	0.002	0.003	0.021

Appendix table 7 TBR2 VFA C-mol

		Acetate	Propionate	IsoButyrate	Butyrate	IsoValerate
Date	Batch	[g/L]	[g/L]	[g/L]	[g/L]	[g/L]
12.05.2025	2B4	0.137	0.008	0.46	0.067	0.023
13.05.2025	2B4	0.168	0.013	0.454	0.06	0.026
14.05.2025	2B4	0.163	0.011	0	0	0.031
15.05.2025	2B4	0.284	0.037	0.039	0	0.049
19.05.2025	2B4	0.85	0.034	0.118	0	0.055
20.05.2025	2B4	1.168	0.022	0.001	0	0.038
21.05.2025	2B4	2.926	0.046	0.017	0	0.078
21.05.2025	2B5	1.948	0.033	0.146	0.005	0.048
22.05.2025	2B5	2.301	0.08	0.137	0.06	0.09
26.05.2025	2B5	4.926	0.026	0	0	0.054
27.05.2025	2B5	8.459	0.006	0.157	0.021	0.081
28.05.2025	2B5	11.674	0.023	0.05	0.039	0.103
28.05.2025	2B5	12.334	0.034	0.049	0.045	0.111
28.05.2025	2B7	2.873	0	0	0	0.033
29.05.2025	2B7	2.805	0	0	0	0.18
30.05.2025	2B7	5.016	0	0.115	0.008	0.047
02.06.2025	2B7	8.319	0.021	0.153	0.04	0.083

Appendix table 8 Gascontent measured with Biogas 5000

Date	Reactor	CH4	CO2	02	H2S	Balance
	B2	50.7	29.6	0.4	64	19.3
26.03.2025	A1	55.7	30.2	0.4	79	13.7
	A2	52.4	29.4	0.3	67	17.8
	B2	55.1	29.2	0.6	65	15.1
01.04.2025	A1	57.9	29.6	0.3	95	12.3
	A2	56.1	29.6	0.3	79	14
	B2	54	29.1	0.4	80	16.4
02.04.2025	A1	57	29.3	0.1	132	13.5
	A2	54.8	29	0.4	91	15.8
	B2	53.6	31	0.4	66	15.1
08.04.2025	A1	55.9	31	0.4	84	12.8
	A2	55.9	31.3	0.1	84	12.6
	B2	52	31	0.4	76	16.7
09.04.2025	A1	53.5	31.1	0.3	88	15
	A2	53.5	31.1	0.3	84	15
	B2	48.4	31.2	0.4	61	19
10.04.2025	A1	49.8	32.5	0.3	86	17.3
	A2	50.7	30.9	0.3	67	18.1
	B2	49.4	33.2	0.4	91	17
17.04.2025	A1	38.8	38.9	0.4	325	21.8
	A2	50.1	32.2	0.4	141	17.5
	B2	52.8	32.9	0.4	91	13.9
23.04.2025	A1	29	42.9	0.4	376	27.8
	A2	54.4	31.7	0.3	110	13.6
	B2	48.8	33	0.4	73	17.9
25.04.2025	A1	23.7	41.5	0.4	446	34.4
	A2	50.7	31.7	0.4	99	17.1
	B2	52.8	31.3	0.4	71	15.6
06.05.2025	A1	26.7	38.1	0.1	308	35.1
	A2	53.6	31.2	0.3	152	14.9
	B2	49.4	31	0.5	62	19.2
08.05.2025	A1	25.8	38.8	0.4	297	35.2
	A2	50.1	31.3	0.3	160	18.2
	B2	52.2	31.6	0.4	95	15.9
13.05.2025	A1	27.7	40.2	0.4	185	31.7
	A2	52.5	30.9	0.3	88	16.3
	B2	50	31.4	0.4	84	18.3
15.05.2025	A1	26.4	39.6	0.4	197	33.6
	A2	49.7	30.4	0.3	75	19.5
	B2	51	32	0.4	66	16.6
21.05.2025	A1	27	39.6	0.4	186	33
	A2	50.6	31.2	0.4	80	17.8
22.05.2025	B2	49.5	32.1	0.4	75	18

	A1	26.4	38.6	0.4	156	34.7
	A2	48.7	30.7	0.3	82	20.9
	B2	53.3	31.9	0.4	70	14.8
27.05.2025	A1	31.6	36.9	0.3	146	31
	A2	54.2	30	0.3	141	15.4
	B2	51.1	32	0.4	137	16.5
28.05.2025	A1	33.5	35.9	0.4	206	30.3
	A2	53.4	29.5	0.3	124	16.9
	B2	53.8	32.9	0.4	76	13.2
03.06.2025	A1	52.3	32.3	0.4	74	14.9
	A2	63.3	28	0.4	87	8.3
	B2	50.5	33.2	0.4	60	15.9
05.06.2025	A1	51.8	31.7	0.4	73	16.2
	A2	59.4	27.5	0.4	69	12.8

Appendix table 9 Statistic test gas content

For low pH		For high pH				
ANOVA:	p = 0.0014	ANOVA:	p = 0.0024			
	F = 7.93		F = 9.26			
Pairwise t-tests:		Pairwise t-tests:				
RRS vs. RRA:	p = 0.019	RRS vs. RRA:	p = 0.197			
RRS vs. RRW:	p = 0.188	RRS vs. RRW:	p = 0.031			
RRA vs. RRW:	p = 0.011	RRA vs. RRW:	p = 0.012			

Appendix table 10 TBR1 TCD data

Study	Hydrogen	vdrogen Carbon dioxide Metha		Methane			
TBR 1	Time	Conc.	Time	Conc.	Time Conc.		Conc.
Date	[min]	[mole-%]	[min]	[mole-%]		[min]	[mole-%]
24.03.2025	2.24	61.98	4.15		28.51	8.99	-
	2.24	57.37	4.15		27.18	8.98	-
	2.24	59.84	4.15		26.72	8.99	-
28.03.2025	2.24	58.17	4.12		23.89	8.96	0.03
	2.24	58.05	4.12		23.38	8.97	0.02
	2.24	56.99	4.12		23.93	8.97	0.02
31.03.2025	2.24	63.16	4.12		24.45	8.97	0.03
	2.24	61.97	4.12		25.08	8.97	0.03
	2.24	57.58	4.12		24.45	8.97	0.03
01.04.2025	2.23	51.69	4.12		23.27	8.97	0.03
	2.24	63.99	4.12		25.66	8.96	0.03
	2.23	43.08	4.12		24.22	8.97	0.03
02.04.2025	2.23	29.99	4.12		22.00	8.97	0.03
	2.23	38.93	4.12		22.93	8.96	0.03
	2.23	28.14	4.12		24.10	8.97	0.03
03.04.2025	2.24	56.39	4.12		29.71	8.97	0.06
	2.24	53.46	4.12		28.58	8.97	0.05
	2.24	56.98	4.12		28.49	8.97	0.05
04.04.2025	2.24	61.22	4.12		26.42	8.97	0.08
	2.24	47.68	4.12		24.55	8.97	0.08
	2.23	38.78	4.12		24.25	8.97	0.07
07.04.2025	2.24	62.87	4.12		25.07	8.97	0.21
	2.23	59.58	4.11		24.58	8.96	0.21
00.04.2025	2.23	62.89	4.11		25.59	8.96	0.21
08.04.2025	2.23	64.51	4.12		25.39	8.96	0.22
	2.23	64.09	4.11		25.93	8.96	0.22
00 04 2025	2.23	61.12	4.12		25.84	8.96	0.23
09.04.2025	2.24	61.53	4.11		28.02	8.98	0.07
	2.24	60.56	4.11		27.88	8.98 8.98	0.07
10.04.2025	2.24	64.46 65.11	4.11		28.2		0.09
10.04.2025	2.24 2.24	75.22	4.12 4.11		29.15 34.93	8.98 8.98	0.17 0.23
	2.24	60.82	4.11		28.34	8.98	0.23
11.04.2025	2.24	61.20	4.14		28.18	8.98	1.30
11.04.2023	2.24	63.26	4.14		28.68	8.97	1.31
	2.24	57.86	4.14		26.94	8.97	1.25
14.04.2025	2.24	55.20	4.14		25.48	8.98	1.64
14.04.2023	2.24	64.67	4.14		26.49	8.97	1.73
	2.24	61.65	4.14		24.17	8.98	1.66
25.04.2025	2.24	61.09	4.14		22.06	8.98	1.90
25.01.2025	2.24	58.92	4.14		25.53	8.98	1.74
	2.24	62.35	4.14		26.81	8.98	1.80
	2.24	02.33	7.17		20.01	0.70	1.00

16.04.2025	2.24	67.74	4.14	31.08	8.98	1.77
	2.24	59.45	4.15	27.25	8.98	1.55
	2.24	59.24	4.15	27.45	8.98	1.55
17.04.2025	2.24	43.68	4.16	26.15	8.97	1.68
	2.24	56.48	4.16	21.76	8.97	2.01
	2.24	56.67	4.16	27.39	8.97	1.81
22.04.2025	0	0	4.16	34.56	8.96	51.73
	0	0	4.16	32.84	8.97	49.80
	0	0	4.16	32.74	8.96	47.86
23.04.2025	0	0	4.16	37.49	8.96	52.70
	0	0	4.16	37.78	8.96	53.80
	0	0	4.16	39.59	8.96	57.30
24.04.2025	2.23	9.96	4.17	21.87	8.96	46.35
	2.23	9.84	4.16	22.75	8.96	46.66
	2.23	9.56	4.17	21.31	8.96	45.29
25.04.2025	2.24	43.87	4.17	12.25	8.97	3.70
23.01.2023	2.24	37.10	4.17	13.12	8.97	6.23
	2.24	43.10	4.17	12.40	8.97	3.81
28.04.2025	2.24	1.39	4.17	30.34	8.97	41.65
20.01.2023	2.24	1.36	4.17	28.60	8.97	39.12
	2.24	1.30	4.17	28.12	8.97	38.83
29.04.2025	2.24	0.11	4.17	34.12	8.97	55.00
27.01.2023	0	0.11	4.17	34.05	8.97	55.02
	2.24	0.17	4.17	34.70	8.97	55.94
02.05.2025	2.24	0.36	4.18	36.58	8.97	53.52
02.03.2023	2.24	0.37	4.17	36.96	8.97	54.30
	2.24	0.37	4.17	38.03	8.97	56.76
05.05.2025	2.24	1.65	4.17	37.31	8.97	55.65
03.03.2023	2.24	1.65	4.18	37.69	8.97	56.63
	2.24	1.59	4.18	36.93	8.97	54.71
06.05.2025	0	0	4.18	36.11	8.97	53.50
00.03.2023		0				
	0	0	4.18 4.18	37.51 36.68	8.97	57.11 55.03
07.05.2025	0	0	4.18	38.07	8.97 8.97	53.05
07.03.2023				22.79		
	0	0	4.18		8.98	30.37
00.05.2025	0	0	4.18	37.49	8.97	53.24
08.05.2025	0	0	4.18	33.78	8.97	47.04
	0	0	4.18	39.02	8.97	55.34
00.05.2025	0	0	4.18	35.45	8.97	50.42
09.05.2025	0	0	4.18	39.62	8.97	55.73
	0	0	4.18	38.55	8.97	54.14
10.05.0005	0	0	4.18	38.80	8.97	56.25
12.05.2025	0	0	4.19	37.36	8.98	53.37
	0	0	4.18	37.71	8.97	53.62
12.05.2025	0	0	4.18	35.25	8.97	50.87
13.05.2025	2.24	0.30	4.18	38.24	8.97	54.61

	2.23	0.30	4.18	38.24	8.97	54.76
	2.23	0.30	4.18	38.31	8.97	54.60
14.05.2025	2.23	1.49	4.2	11.26	9	0.64
1 1105.2025	2.23	1.44	4.19	11.35	9	0.66
	2.24	1.62	4.2	10.26	9	0.64
15.05.2025	2.23	1.84	4.2	28.32	8.98	45.16
10.00.2020	2.23	2.03	4.19	27.91	8.98	44.99
	2.24	2.01	4.19	32.50	8.98	51.50
16.05.2025	2.24	0.32	4.19	30.07	8.98	51.44
	0	0	4.19	31.98	8.98	50.04
	0	0	4.19	32.88	8.98	51.65
19.05.2025	0	0	4.19	37.60	8.98	54.87
	0	0	4.19	37.74	8.98	55.16
	0	0	4.19	34.96	8.98	52.39
20.05.2025	0	0	4.19	38.81	8.98	56.95
	0	0	4.19	34.79	8.98	49.60
	0	0	4.19	36.28	8.98	54.73
21.05.2025	0	0	4.19	36.42	8.98	52.12
	0	0	4.19	35.99	8.98	55.41
	0	0	4.2	35.94	8.98	52.05
22.05.2025	0	0	4.19	35.99	8.98	50.54
	0	0	4.2	34.10	8.98	47.87
	0	0	4.2	30.76	8.98	51.04
23.05.2025	0	0	4.2	36.45	8.98	55.54
	0	0	4.2	35.93	8.98	55.10
03.06.2025	0	0	4.21	35.99	8.99	53.31
	0	0	4.21	36.88	8.99	55.49
	0	0	4.21	35.85	8.99	55.77
04.06.2025	0	0	4.21	38.12	8.99	57.28
	0	0	4.21	36.44	8.99	56.36
	0	0	4.21	39.31	8.99	59.24
05.06.2025	0	0	4.21	35.96	8.99	54.88
	0	0	4.21	37.12	8.99	56.98
	0	0	4.22	38.00	8.99	58.51

Appendix table 11 TBR2 TCD data

TBR2	Acetate	Hydrogen		Carbon dioxide			
Study		Time			Conc.	Time	Conc.
Date	[g/L]	[min]	[mole-%]	[min]	[mole-%]	[min]	[mole-%]
12.05.2025	0.137	2.24	0.36	4.20	1.99	8.98	0.31
		0	0.00	0.00	0.00	8.99	0.30
		2.24	0.30	0.00	0.00	8.99	0.30
13.05.2025	0.168	2.25	76.90	4.20	7.80	8.99	0.36
		2.25	74.76	4.20	6.90	8.99	0.35
		2.25	70.38	4.19	5.77	8.99	0.33
14.05.2025	0.163	2.25	78.11	4.21	4.28	9	0.35
		2.25	66.88	4.21	4.40	9	0.35
		2.25	81.37	4.21	4.35	9	0.35
15.05.2025	0.284	2.25	56.56	4.21	4.04	9	0.40
		2.25	81.29	4.21	5.07	9	0.42
		2.25	80.24	4.21	5.21	9	0.42
16.05.2025	0.3972	2.24	22.07	4.22	4.44	9	0.51
		2.24	34.18	4.21	5.08	9	0.45
		2.25	71.48	4.20	6.40	9	0.51
19.05.2025	0.85	2.25	78.99	4.20	4.57	9	1.98
		2.25	73.92	4.21	4.69	9	1.95
		2.25	74.08	4.20	4.67	9	1.96
20.05.2025	1.168	2.25	76.09	4.20	5.32	9	4.62
		2.25	69.87	4.20	5.19	9	4.37
		2.25	77.34	4.21	5.23	9	4.70
21.05.2025	1.948	2.25	68.75	4.21	4.31	9	9.36
		2.25	64.48	4.20	4.32	9	9.16
		2.25	69.98	4.22	5.23	9	9.33
22.05.2025	2.55	2.24	43.91	4.22	4.03	8.99	19.64
		2.24	40.48	4.2	3.80	8.99	18.52
		2.24	40.15	4.21	3.51	8.99	18.16
23.05.2025	3.738	2.24	13.32	4.21	3.96	8.99	42.13
		2.24	13.96	4.21	0.28	8.99	44.03
		2.24	12.91	0	0.00	8.99	42.25
03.06.2025	6.8795	0	0	0	0.00	8.98	81.81
		0	0	0	0.00	8.98	85.30
		0	0	0	0.00	8.98	86.49
04.06.2025	10.021	0	0	4.21	4.54	8.98	87.37
		0	0	0	0.00	8.98	84.96
		0	0	0	0.00	8.98	87.32
05.06.2025	12.305	0	0	4.22	4.42	8.98	88.35
		0	0	0	0.00	8.98	89.05
		0	0	4.22	4.07	8.98	86.33